

THESIS

THRESHOLDS FOR RUNOFF GENERATION IN EPHEMERAL STREAMS
WITH VARYING MORPHOLOGY IN THE SONORAN DESERT IN ARIZONA, USA

Submitted by

Joshua D. Faulconer

Department of Ecosystem Science and Sustainability

In partial fulfillment of the requirements

For the Degree of Master of Science

Colorado State University

Fort Collins, Colorado

Spring 2015

Master's Committee:

Advisor: Stephanie Kampf

Lee McDonald

Michael Ronayne

Copyright by Joshua D. Faulconer 2015

All Rights Reserved

ABSTRACT

THRESHOLDS FOR RUNOFF GENERATION IN EPHEMERAL STREAMS WITH VARYING MORPHOLOGY IN THE SONORAN DESERT IN ARIZONA, USA

In ephemeral streams, infrequent surface flow can be the main source of water that sustains plants throughout long dry periods. The objectives of this research are to: (1) explore seasonality of rainfall runoff in different channel types and (2) examine how runoff thresholds vary by channel type. The study area was two watersheds with areas of 188 km² and 323 km² on the Yuma Proving Grounds (YPG) in the Sonoran Desert near Yuma, Arizona. Eight tipping bucket rain gauges were installed to measure precipitation. Runoff was measured with 18 pressure transducers in five different channel types with different channel morphologies and contributing areas ranging from 0.002 km² to 225 km². Over approximately two years there were 11 to 48 rain events at the different rain gauges. Stream types with bedrock channels and small watershed areas between 0.005 km² and 0.015 km² produced runoff when the peak 60-minute precipitation intensity (I₆₀) exceeded 4-6 mm hr⁻¹. At these sites, 17-25 percent of the rain storms generated runoff. I₆₀ values of 5-9 mm hr⁻¹ produced runoff in streams with contributing areas of 0.021-0.061 km² on mid-Pleistocene piedmont surfaces covered by desert pavement. At these sites, 31-36 percent of rain events produced runoff. Streams incised into bedrock with some alluvium fill produced runoff at larger I₆₀'s of 13-18 mm hr⁻¹. Contributing areas for these sites were 0.8 km² to 2.2 km², and up to 10 percent of precipitation events at these sites produced flow. Precipitation thresholds for runoff generation in streams with contributing areas >3 km² were not clearly defined due to the influences of variable precipitation in upstream tributaries and transmission losses of streamflow through channel bed alluvium. For watersheds with <3km², rain intensity thresholds

increased with the log of catchment area, and as a result flow frequency tended to decrease with increasing catchment area.

ACKNOWLEDGMENTS

The author wishes to thank Dr. Stephanie Kampf for her continuous and generous support, advisement, and edits; without her patience and guidance this document might never have been completed. The author also thanks Jeremy Shaw for his support, his help in the field and at the computer, his generous sharing of knowledge, and his never-ending willingness to discuss the topic. Dr. David Cooper – the lead PI – gave insights and support, without him the author would not have had the opportunity to be part of this research and wonderful team. Lee MacDonald liberally marked edits and comments on the defended version of this document, which greatly helped the author hone the thesis into its final form. The author also thanks his father, Keith Faulconer, for taking time off work, driving 1300 miles round trip, and spending a week in the brutal desert doing grueling work at the whip of the author’s tongue. Andrew Carlson was a great help in the field and the lab. The author’s mother, Sheryl Faulconer, was always there with support, and she is greatly appreciated. The Lee and Hillary MacDonald Scholarship provided the author with some helpful living and school supply funds. This research was funded by The Strategic Environmental Research and Development Program (SERDP) through grant RC-1725.

TABLE OF CONTENTS

ABSTRACT.....	ii
ACKNOWLEDGEMENTS.....	iv
1. INTRODUCTION.....	1
2. BACKGROUND.....	2
3. STUDY AREA.....	4
3.1. Stream classification.....	6
3.2. Study design.....	8
4. METHODS.....	13
4.1. Data collection.....	13
4.2. Drainage area characteristics.....	15
4.3. Data analysis.....	16
5. RESULTS.....	20
5.1. Seasonality of rain.....	20
5.2. Rainfall-runoff events.....	22
5.3. Selection of rain event metrics for threshold analysis.....	30
5.4. Runoff thresholds by channel type.....	32
6. DISCUSSION.....	43
6.1. Runoff thresholds.....	43
6.1.1. Channels <3 km ²	43
6.1.2. Incised Alluvium channels.....	46
6.1.3. Braided channels.....	48
6.2. Runoff frequency.....	49
6.3. Uncertainty.....	51
6.3.1. Minimum Inter-event Times (MIT).....	51
6.3.2. Winter storm effects.....	52
6.3.3. Lag times.....	53
7. CONCLUSIONS.....	55
8. REFERENCES.....	57

1. INTRODUCTION

Arid and semi-arid regions make up 41% of the earth's land area, and in 2005 more than 2 billion people out of the 6.5 billion world human inhabitants lived in these regions (Millennium Ecosystem Assessment 2005). Climate change is increasing the amount of area classified as arid, and anthropogenic land use continues to degrade lands and increase areas of desertification. The majority of biodiversity in arid regions is found in the riparian regions (Shaw and Cooper, 2008; Levick, 2008) since inter-channel arid soils receive limited precipitation and often have low infiltration values (Hogan et al. 2004).

Runoff in ephemeral stream channels is typically caused by high intensity precipitation that produces infiltration excess overland flow on the inter-channel soils and bedrock. Channel transmission losses can be substantial in ephemeral streams, and some studies report that these losses increase with increased catchment area due to transmission losses through the channel network (Simanton and Osborn, 1983; Goodrich et al., 1997). These losses along the channel make it difficult to predict when and where ephemeral channels will flow, and a better understanding is needed of how runoff occurrence relates to varying channel morphology and contributing area size.

In ephemeral streams, infrequent surface flow can be the main source of water that sustains plants throughout long dry periods, so an understanding of the runoff processes and precipitation characteristics that lead to flow is important to understanding these ecosystems. Prior research suggests that runoff generation in arid ephemeral streams is a threshold-like process, with runoff occurring only during storms above a threshold precipitation intensity (Kidron and Pick, 2000; Yair and Lavee, 1985). This research aims to: (1) explore seasonality of rainfall runoff in different channel types and (2) examine how runoff thresholds vary by channel type. Understanding the rain thresholds that produce runoff will help researchers predict how changes in precipitation will affect both runoff and the water it provides to riparian ecosystems in arid environments.

2. BACKGROUND

Storms that produce runoff in arid regions are usually highly localized, short duration, high intensity convective storms (Osborn, 1964). The scarcity of rainfall and limited rainfall depth in short storms generally preclude subsurface flow and the development of saturated areas, so saturation overland flow is not common in arid regions (Yair and Lavee, 1985). High rainfall intensity instead leads to infiltration-excess overland flow (Wilcox et al., 1997), and in arid regions precipitation intensity is more correlated with runoff production than precipitation depth or duration (Osborn, 1964; Osborn and Lane 1969; Simanton and Osborn, 1983; Yair and Lavee, 1985; Syed et al., 2003). Convective storms with high intensity precipitation typically have high spatial variability, and the location of the storm core within a watershed affects the amount of runoff production (Syed et al., 2003).

Development of infiltration excess overland flow on desert land surfaces also relates to the land cover types, such as bedrock and desert pavement, that have low permeability (Springer, 1958; Yair and Lavee, 1985). Desert pavement consists of a one or two-particle thick layer of closely packed, angular to sub-rounded, darkly varnished cobble surface overlaying an A horizon layer of eolian fines a few centimeters deep with low permeability (Springer, 1958; McFadden et al., 1987). Desert pavement is widely distributed in arid regions of the western United States (Turk and Graham, 2011). In the Sonoran Desert the eolian fines horizon of desert pavement has been reported to have a very low infiltration rate of less than 1 cm hr^{-1} (McDonald et al., 2004). This horizon can be a critical regulator of infiltration (Springer, 1958; Turk and Graham, 2011; Young et al., 2004).

In contrast to bedrock and desert pavement, ephemeral stream channels are composed of unconsolidated alluvium with high permeability (Yair and Lavee, 1985). Once runoff reaches the channel network, transmission losses of surface flow to the underlying alluvium are common. Transmission loss in ephemeral channels can reduce the flow volume and peak discharge downstream (Osborn and Lane,

1969; Simanton and Osborn, 1983; Yair and Lavee, 1985). Osborn and Lane (1969) reported that runoff from small watersheds is much greater per unit area than runoff from larger complex watersheds. This is at least partly due to larger watersheds having more channel transmission losses, particularly in downstream reaches (Simanton and Osborn, 1983; Goodrich et al., 1997). Spatial and temporal connectivity of the drainage network is rare except in the most extreme runoff events (Jaeger and Olden, 2012) because of both transmission losses and partial area storm coverage (Goodrich et al., 1997). Flow discontinuity increases in large watersheds due to increased channel widths and depth of alluvium (Yair and Lavee, 1985). Convective cells can move on the order of 100 times greater than flow velocities, thus preventing runoff generation from occurring simultaneously over the entire area covered by rain (Yair and Lavee, 1985).

Because of the short duration of runoff-producing convective storms, Osborn (1964) concluded that 15, 30, and 60-minute intensities are important when comparing rain to runoff. On average 66% of a convective storm's rain falls in the first 15 minutes, 90% in 30 minutes, and 100% in an hour (Osborn, 1964). Other studies have identified 5-minute (Schreiber and Kincaid, 1967) and 15-minute rainfall intensities (Osborn and Lane, 1969) to be the dominant variables for determining runoff volume and peak flow. Ranges of runoff-producing rainfall thresholds have been identified in prior studies in arid and semi-arid environments. In Israel rain intensities of 9 mm hr^{-1} produced runoff in 45 minutes, and 12 mm hr^{-1} produced runoff in 30 minutes (Yair and Lavee, 1985). Goodrich et al. (1997) and Syed et al. (2003) used 10-minute intensities of greater than 25 mm hr^{-1} as their designation of a storm core because they determined that this intensity was a conservative estimate for producing runoff. The current study expands on these prior studies by examining how precipitation thresholds for runoff generation are affected by stream morphology and size of contributing area.

3. STUDY AREA

The study location is in the Northern Sonoran Desert on the United States Army Yuma Proving Grounds (YPG) in the southwest corner of Arizona in the Southwest United States (Figure 3.1). This region of the Sonoran Desert has a mean aridity index of 0.047, which makes it hyper-arid (Howe 2013). YPG's mean annual precipitation from 1958-2010 was 90 mm (Western Regional Climate Center, 2013), and this precipitation falls primarily during two seasons. During the winter months of November to March frontal systems from the Pacific Ocean bring low intensity, long duration rains that cover a large area (Hallack-Alegria and Watkins, 2007). During the summer months of July to September the North American monsoon (NAM) causes short duration, high-intensity convective thunderstorms covering no more than a few tens of square kilometers (Hallack-Alegria and Watkins, 2007). Pacific Ocean tropical storms can also bring rain during the summer.

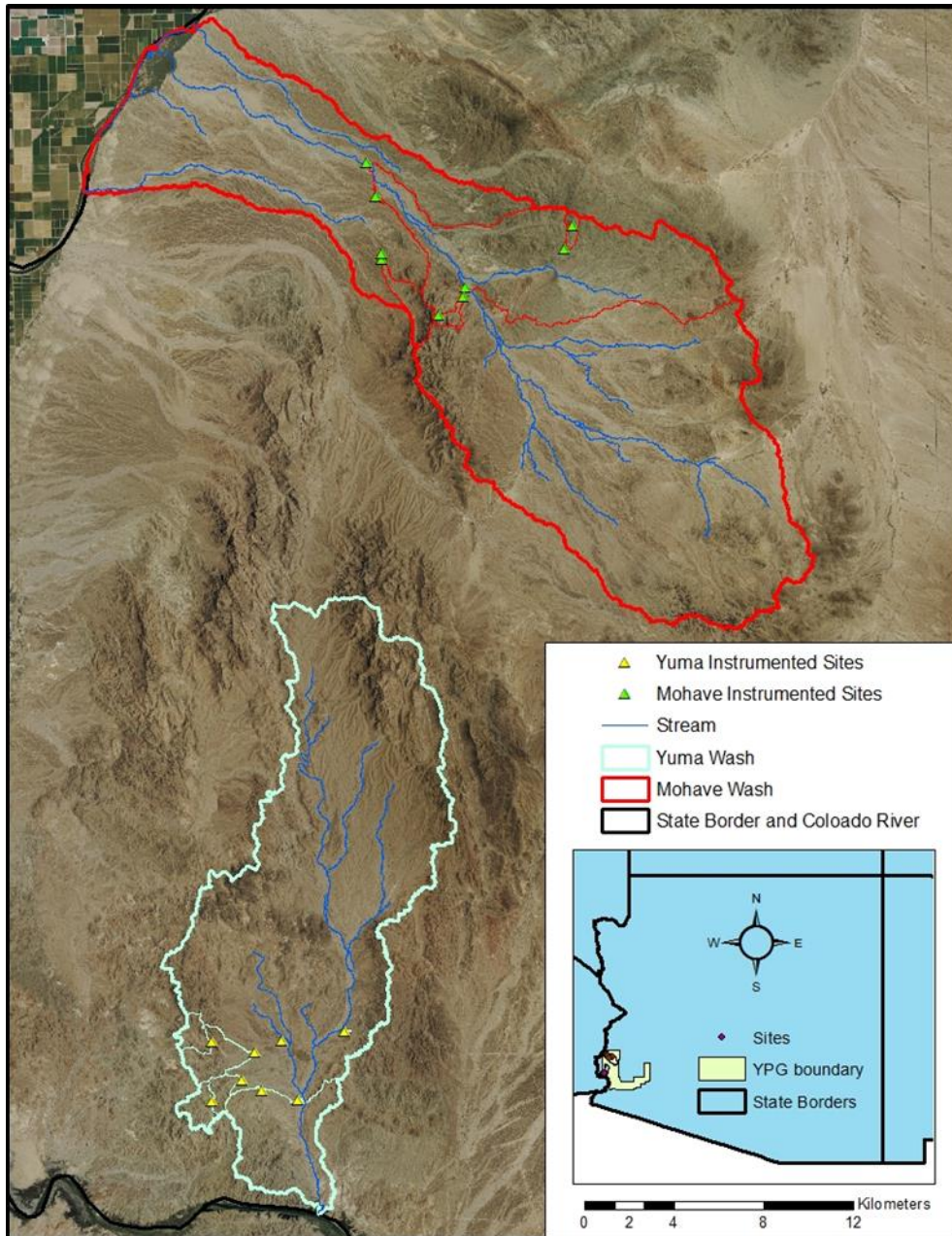


Figure 3.1. Map of study area with the outline of the two study watersheds and locations of instrumented sites.

The two study watersheds are Yuma Wash and Mohave Wash (Figure 3.1), which drain into the Colorado River. Yuma Wash drains to the south, and Mohave Wash drains to the northwest. Yuma Wash is 28 km long and has a drainage area of 188 km². Mohave Wash is 37 km long with a drainage area of 323 km². Bedrock is exposed mainly in the jagged mountains of the study watersheds, with the lowland

valleys filled with alluvium. Gently sloping alluvial fans fill in most of the areas between the exposed bedrock and lowland alluvium and are termed piedmont surfaces in this study. Piedmont surfaces are depositional surfaces that are stable and have formed desert pavement. The upper piedmont is the area at the base of the present day mountains.

Bedrock in the study area is mostly intrusive and extrusive igneous with some marine layers. Most of the bedrock in Yuma Wash is rhyolite (47% of total watershed area), with 12% sandstone 7% granite, and 4% amphibolite (Arizona Geological Survey (AGS), 2000). The remaining 30% of the area is covered by alluvium. In Mohave Wash rhyolite covers only 20% of the watershed area; granite and sandstone cover 10% and 2% of the watershed area, respectively, and the remaining 68% is alluvium (Arizona Geological Survey (AGS), 2000).

Desert pavement areas have limited vegetation with the exception of creosote bush and cacti, such as *Fouquieria splendens* (ocotillo), *Carnegiea* (saguaro), and *Opuntia* (cholla). Vegetation is more abundant and diverse in the riparian zone, with species types including *Cercidium* spp. (palo verde), *Olneya tesota* (iron wood), *Prosopis* spp. (mesquite), *Larrea tridentata* (creosote bush), *Ambrosia dumosa* (white bursage), *Pleuraphis rigida* (big galleta grass), ocotillo, and *Krameria grayi* (white ratany), with most of the biomass as ironwood, palo verde, and creosote bush (McDonald et al., 2004; Sutfin, 2014).

3.1. Stream classification

The geomorphic stream classification presented in Sutfin et al. (2014) was used in this research to select the study sites. This classification divides the fluvial system into five morphologically distinct stream types: Piedmont Headwater, Bedrock, Bedrock with Alluvium, Incised Alluvium, and Braided (Table 3.1). These channel types represent a downstream progression from the mountain headwaters and piedmont surfaces to the valley bottoms, with the headwater channels incised into either the

bedrock or piedmont surfaces. Further downstream the stream channels have gravel- to cobble-sized alluvium in the channel beds, and these channels have incised into the sand to cobble-sized Pleistocene alluvial valley bottoms. The width and depth of alluvium in the channel beds tends to increase downstream. All of the channels in the study area are ephemeral.

Table 3.1: Channel types, locations, descriptions, and corresponding abbreviations for each study watershed defined by Sutfin (2013).

Channel Type	Location	Description	Abbreviation
Piedmont Headwaters	Piedmont	Small channels incised into the desert pavement. Confined by unconsolidated alluvium.	PH
Bedrock	Headwaters in the mountains	Cut into exposed bedrock. Void of persistent alluvium.	BK
Bedrock with Alluvium	Upper piedmont	Partially confined by bedrock. Enough persistent alluvium to create bedforms.	BA
Incised Alluvium	Piedmont	Incised into the piedmont's unconsolidated alluvial material.	IA
Braided	Alluvial basins between mountain ranges	Large, multithreaded channels.	BD

3.2. Study design

Stage was measured at 18 locations that represent the range of channel geomorphic classifications in Table 3.1. In Table 3.2, stream stage sites are grouped by channel geomorphic type (Sutfin et al., 2014) with the exception of MIA1. Although MIA1 is a single threaded Incised Alluvium channel at the study reach, it has a braided reach upstream and a basin area size closer to the Braided channel types, so it was grouped with the Braided channels. Each watershed had 4 rain gauges and 9 runoff-monitoring sites, two of each channel type except Braided channels, which only had one runoff-monitoring site. Braided channels only had one monitoring location because each watershed has only one main stem braided channel. Flow depths were also difficult to measure in these channel types since they are wide multi-thread channels where flow events do not consistently pass through the same section of channel. The M or Y preceding the channel type abbreviation in Table 3.2 indicates if the site is in Mohave Wash (M) or Yuma Wash (Y). Piedmont Headwater (PH) channel types have the smallest contributing areas and shortest stream lengths, with contributing areas of 0.002 to 0.049 km² and contributing stream lengths of 0.01 to 1.16 km (Table 3.2). Bedrock (BK) channel sites have only slightly larger contributing areas and stream lengths, with contributing areas of 0.005 to 0.093 km², and stream lengths of 0.04 to 1.62 km. Bedrock with Alluvium (BA) sites have larger contributing areas of 0.8 to 2.2 km² and stream lengths of 16.3 to 35.6 km. Further downstream are the Incised Alluvium (IA) sites, with contributing areas of 3.0 to 5.7 km² and stream lengths of 60.3 to 99.8 km. Furthest downstream are the Braided (BD) channels, including MIA1, with contributing areas of 170 to 225 km² and stream lengths of 3079 to 4211 km.

Table 3.2: Stream stage measurement sites with contributing area, stream length, channel width, and site elevation. If the site is in Yuma Wash the channel type abbreviation is preceded by a Y and is preceded by an M if the site is in Mohave Wash.

Site	Area (km ²)	Stream Length (km)	Channel Width (m)	Site elevation (m)
Piedmont Headwaters				
YPH1	0.021	0.37	1.9	156
YPH2	0.002	0.01	1.4	154
MPH1	0.061	1.16	no data	226
MPH2	0.049	1.02	3.0	242
Bedrock				
YBK1	0.005	0.04	no data	225
YBK2	0.013	0.32	1.7	166
MBK1	0.093	1.62	2.9	464
MBK2	0.015	0.40	1.4	384
Bedrock with Alluvium				
YBA1	2.2	35.6	10.1	211
YBA2	1.7	30.9	7.7	207
MBA1	0.9	18.4	7.1	279
MBA2	0.8	16.3	4.1	328
Incised Alluvium				
YIA1	3.6	60.3	21.9	176
YIA2	5.7	99.8	22.8	162
MIA2	3.0	63.6	9.7	249
Braided				
MIA1	170	3190	38.7	270
YBD1	170	3079	124.1	116
MBD1	225	4211	113.8	201

Figures 3.2-3.6 show examples of the different types of channels and contributing areas. Piedmont Headwater and Bedrock channels are narrow, between 1.4 and 3 m wide, and have little to no alluvium (Table 3.2, Figures 3.2-3.4). Most of the vegetation on the piedmont grows in Piedmont Headwater channels, where the desert pavement is eroded exposing the Pleistocene alluvium (Figure 3.2). Bedrock with alluvium channels are typically 4 to 10 m wide with alluvium filling the base of the channel from bank to bank (Figures 3.3-3.4). Incised Alluvium channels are 10 to 23 m wide with vegetation typically near or on the banks, and they may have some vegetation within the channel (Figures 3.5-3.6). YIA1 has a piedmont headwater channel contributing directly upstream and on the

same side of the IA channel as the YIA1 pressure transducer (Figure 3.6). Braided channels are multi-threaded channels that span widths up to 124 m, with vegetation growing between active channel threads (Figure 3.2).

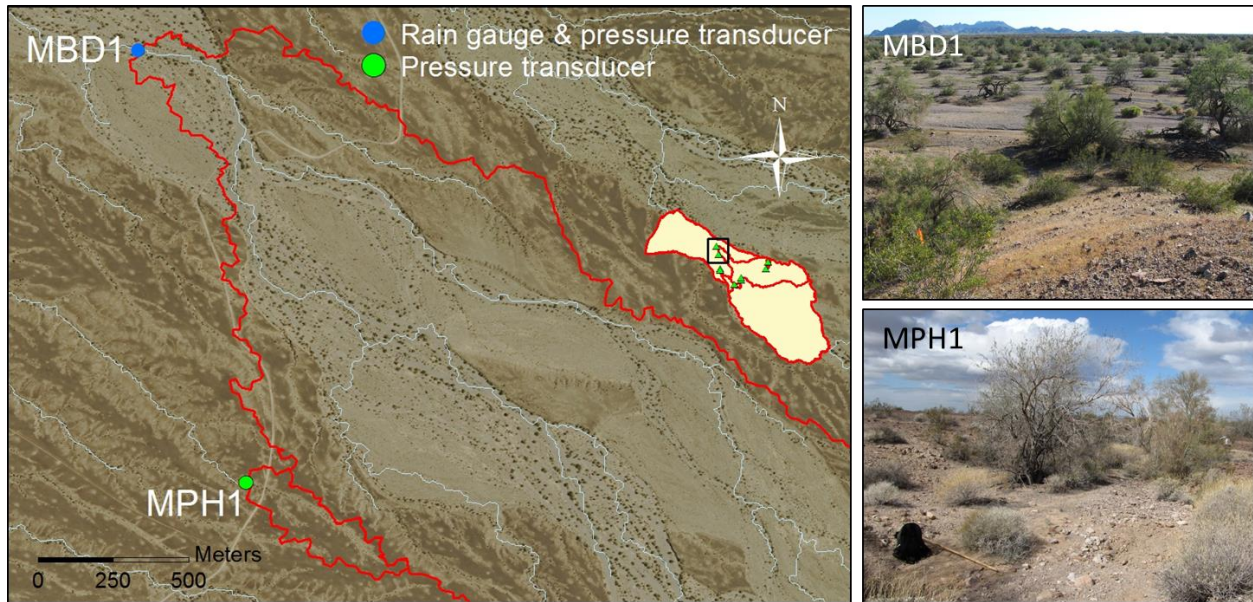


Figure 3.2. Site location, contributing area boundaries, and photographs for MBD1 and MPH1.

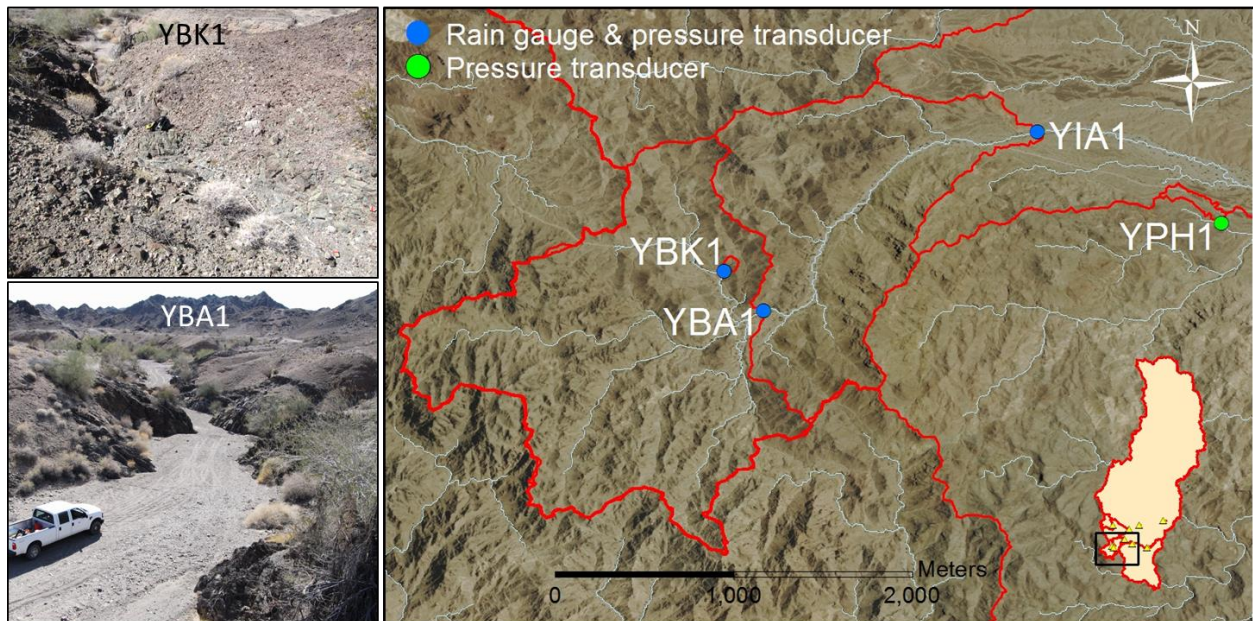
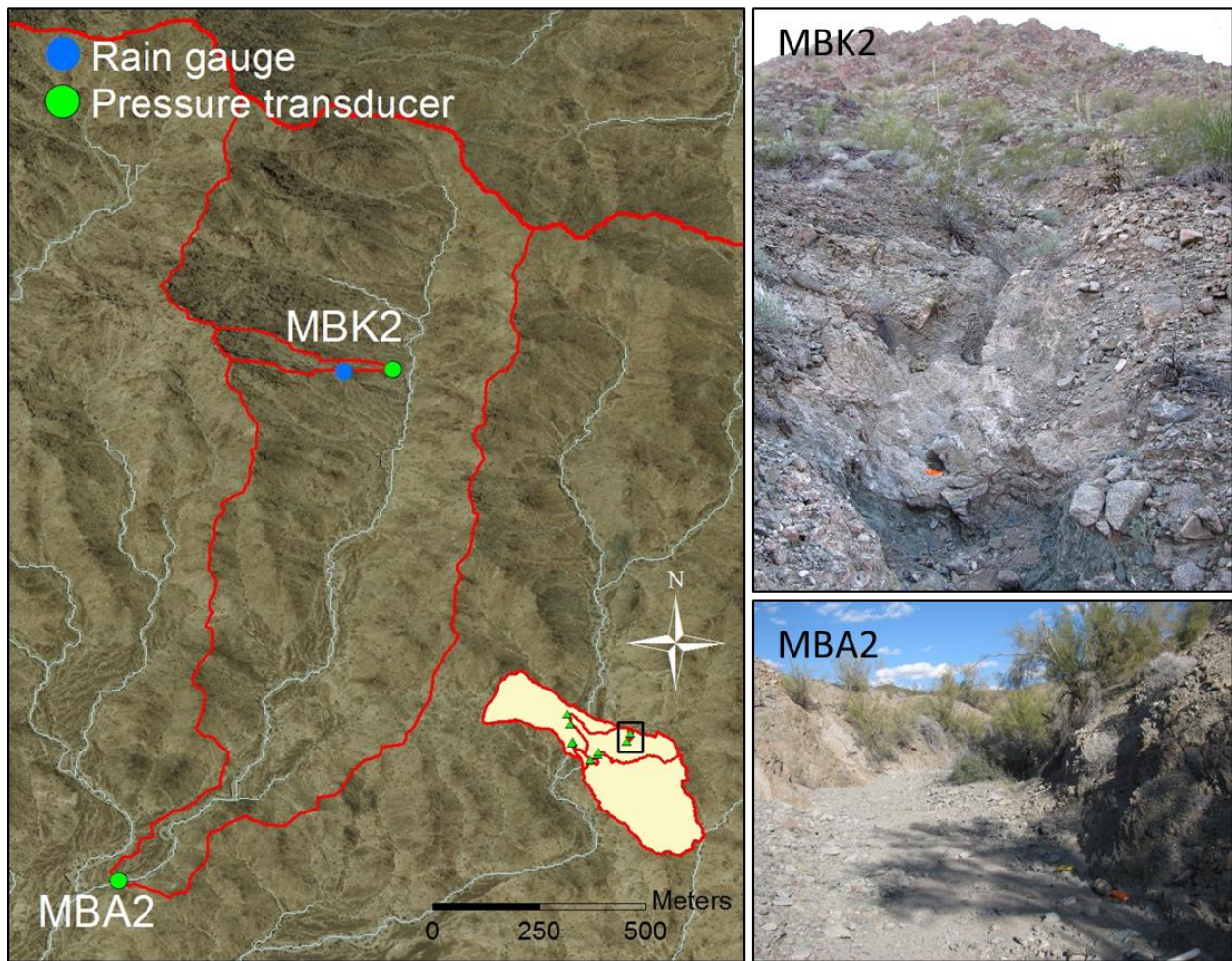


Figure 3.3. Site location and contributing area boundaries for YPH1, YBK1, YBA1, and YIA1. Photographs of YBK1 and YBA1.



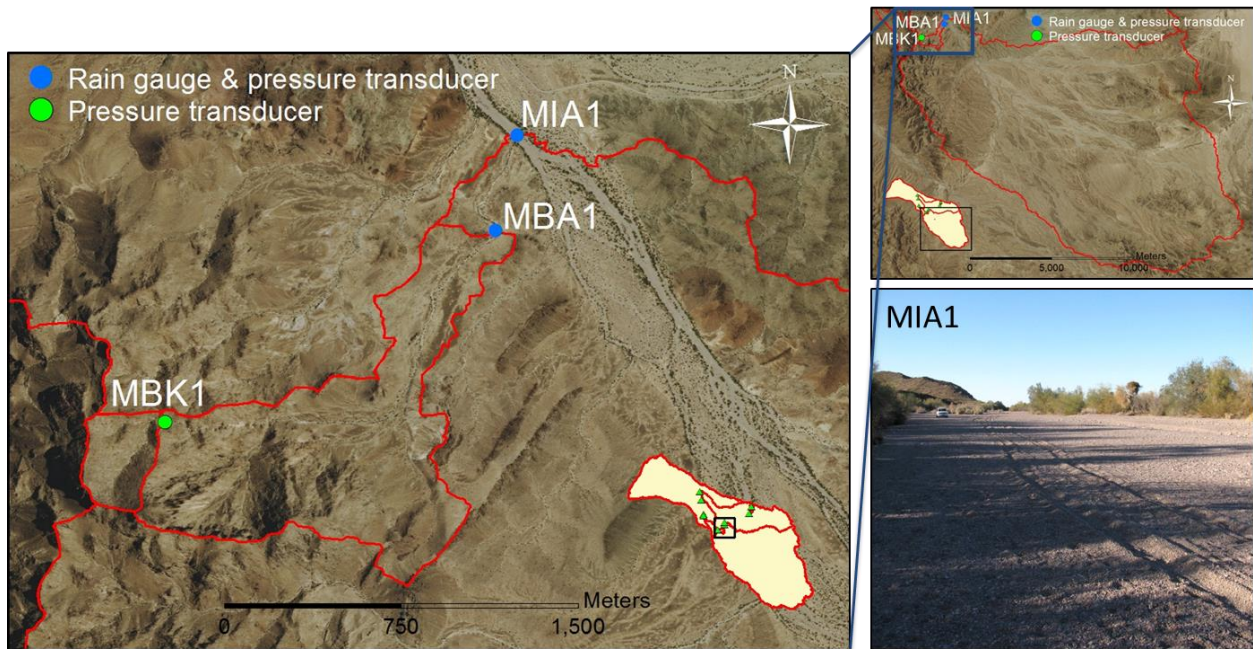


Figure 3.5. Site location and contributing area boundaries for MBK1, MBA1, and MIA1. Photo of MIA1.

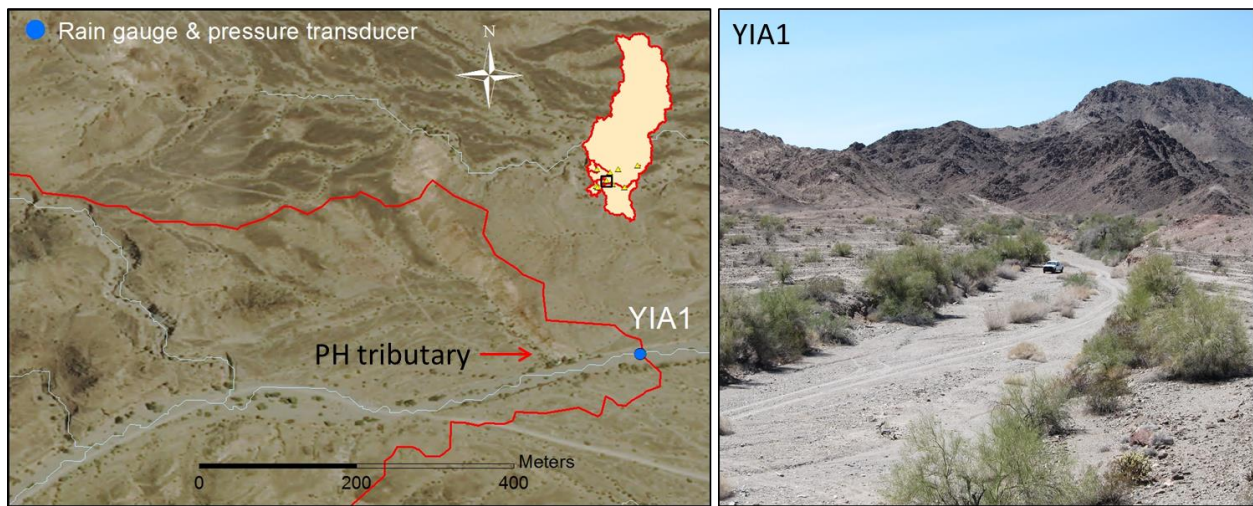
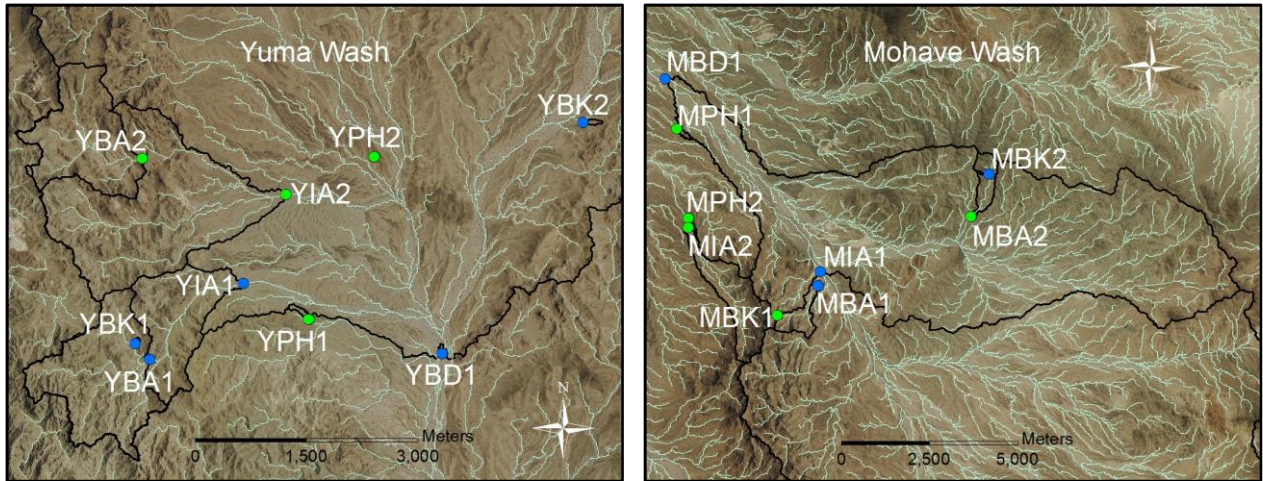


Figure 3.6. Site location and picture of YIA1. Upstream PH tributary shown on map.

4. METHODS

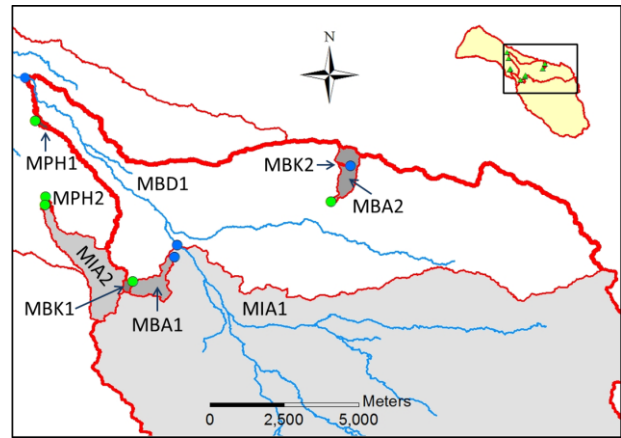
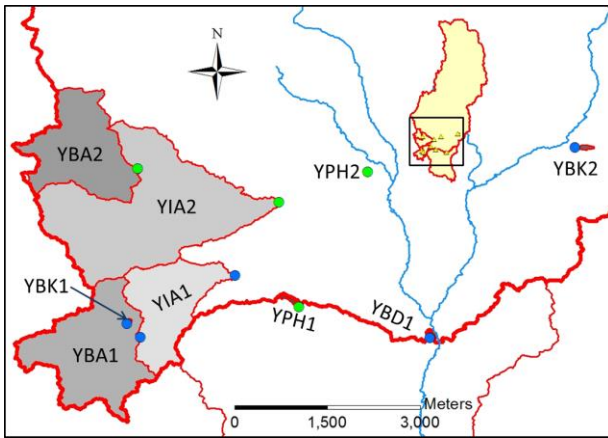
4.1. Data collection

To examine precipitation thresholds for runoff generation in channels with different morphologies, a network of precipitation and stream stage measurements was installed in the two watersheds (Figure 4.1). Each watershed has four rain gauges and nine pressure transducers for monitoring stream stage (Figure 4.1). Precipitation was monitored with either RG3-M tipping-bucket rain gauges, which measured 0.2 mm per tip, and recorded with Onset HOBO Pendant Event loggers (Figure 4.2.A) or TE525 and TB4 tipping bucket rain gauges that measured 0.254 mm per tip and were logged by Campbell dataloggers. Sites with Campbell dataloggers also had subsurface water content measurements as part of related research on subsurface water dynamics. In-Situ Inc. Rugged TROLL 100 pressure transducers were installed in channel beds to measure surface runoff. The pressure transducers at each site were placed inside vented PVC pipe for protection and bolted into bedrock or trees to keep them in place during flow events (Figure 4.2.B). The Rugged TROLL 100 pressure transducers must be used in conjunction with a barometric pressure logger (barologger) in order to subtract out the barometric fluctuations from the water level changes. An In-Situ Inc. Rugged BaroTROLL was placed at the braided site in both watersheds. Point values were continuously logged in 15-minute time steps.



A.

B.



C.

D.

- Rain gauge & pressure transducer
- Pressure transducer

Figure 4.1. Yuma Wash (A and C) and Mohave Wash (B and D) instrument locations. Images A and B are ortho-photographs with black contributing area boundary lines and the names of the instrumented locations. Maps B and D show the contributing areas shaded in grey scale with the site names placed within each contributing area above a pressure transducer monitoring site. Blue dots indicate sites with rain gauges and pressure transducers. Green dots are sites with just pressure transducers.



A.



B.

Figure 4.2. Photographs of (A) the RG3-M stand-alone tipping bucket rain gauge with Onset HOBO Pendant Event logger at YBK2 and (B) pressure transducer inside PVC pipe anchored to an Ironwood at YIA2.

4.2. Drainage area characteristics

The contributing area to each pressure transducer was delineated using the D8 flow direction algorithm in ArcGIS's hydrology tools with 3.6 meter DTMs (Digital Terrain Models) from YPG. The length of channel that could potentially lead to infiltration losses was also calculated by assuming a threshold of 100 cells or 0.0013 km² for channel initiation. This threshold was selected by iteratively testing thresholds of flow accumulation to determine which best corresponded to visually distinguishable channels in ortho-photographs obtained from the U.S. Department of Agriculture's Farm Service Agency's National Agriculture Imagery Program (NAIP imagery obtained from the Aerial Photography

Field Office, June 9, 2013). The stream length was estimated by counting the number of cells with contributing areas above this threshold and multiplying the count by the length of a cell edge.

4.3. Data analysis

To link runoff events with precipitation characteristics, the precipitation record was divided into storm events by assuming a minimum inter-event time (MIT) of 7 hours between tips of a rain gauge. This MIT value was selected based on both the site data and prior research. The longest flow duration recorded in the study was 6.5 hours, slightly shorter than the MIT selected. MIT values of 6-8 hours were also used in over a quarter of the 26 published articles reviewed by Dunkerley (2008). To test the influence of MIT on study results, analyses were also computed using alternate MITs. Rain events of two tips or less of the rain gauge tipping bucket were excluded from the analyses. The rain start time, peak, and end time were identified for each rain event, and four precipitation metrics were calculated for each event at each site: total event magnitude (Depth) and 15, 30, and 60-minute peak intensities (I15, I30, I60).

Table 4.1: Stream stage measurement sites with the site location, distance, and elevation difference to the nearest rain gauge. Some sites were not used for threshold analysis because of data problems, rain gauge distance, or elevation difference. PT stands for pressure transducer.

Site	Rain gauge	Distance to rain gauge (km)	Elevation difference: PT and rain gauge (m)	Used in threshold analysis
Piedmont Headwaters				
YPH1	YIA	1	-19	Yes
YPH2	YIA	2.5	-21	No ¹
MPH1	MBD	1.5	19	Yes
MPH2	MBA	4.2	-38	No ¹
Bedrock				
YBK1	On site until 2/10/2013 then YBA	0.3	16	Yes
YBK2	On site	0	-3	Yes
MBK1	MBA	1.4	184	No ²
MBK2	On site	0	-36	Yes
Bedrock with Alluvium				
YBA1	On site	0	1	Yes
YBA2	YIA	2.2	31	No ¹
MBA1	On site	0	-1	Yes
MBA2	MBK5	1.3	-92	Yes
Incised Alluvium				
YIA1	On site	0	0	Yes
YIA2	YIA	1.4	-14	Yes
MIA2	MBA	4	-31	No ¹
Braided				
MIA1	On site	0	-1	Yes
YBD1	On site	0	1	Yes
MBD1	On site	0	-6	Yes

1. Rain gauge >1.5 km away
2. Elevation change to rain gauge too great

Pressure transducer stream stage data were analyzed to identify flow events. Most flow events were easily distinguished from background noise after correcting for barometric pressure, and converting the pressure transducer data to depth. However, residual noise in the data made it difficult to discern small flow events. To distinguish potential flow events from background noise, cumulative distribution functions (CDFs) were created from the stage data at each site. The CDFs were intended to bring out the highest stage values, which likely correspond to flow events. Stage depths for quantiles of 0.995 and greater were identified, graphed, and visually analyzed for hydrograph features. The dates and times were compared to the rainfall data to determine whether the high stage values were runoff events or noise. Once flow events were identified, the start time, peak, and end of each hydrograph were determined for each flow event.

The stream hydrographs from each site were compared to the nearest rain gauge (Table 4.1) to determine precipitation event characteristics for each flow occurrence at each site. If a rain gauge was not located on the site with the pressure transducer then the closest working rain gauge was used. The lag time between peak precipitation and peak flow was determined. Preliminary data analysis showed poor correspondence between precipitation and flow event records for stream channels that did not have rain gauges within 1.5 km, so YPH2, MPH2, YBA2, and MIA2 were excluded from the threshold analysis (Table 4.1). The correlation between MBK1 flow and the nearest rain gauge (MBA1, 1.4 km) was also poor, with flows produced during low intensity rains and high intensity rains not producing flow. This may be due to the 184 meter difference in elevation between the stream stage site and corresponding rain gauge (Table 4.1), so this site also was excluded from threshold analysis. Both equipment failure and installation timing led to a few cases where the closest rain gauge did not have data for a runoff event. If the closest rain gauge was not recording during the time of the flow, then the next closest rain gauge was used if it was within 1.5 km. If no rain gauge within that distance was recording during a flow event, the flow event was excluded from further analysis. Two runoff events at

MPH (9/6/2013 and 9/2/13) and one runoff event (8/17/12) at YBD were taken out due to no rain gauges in the 1.5 km radius recording at the time of flow. One runoff producing rain event on 12/13/2012 was not recorded for an unknown reason at YBK, so the rain gauge at YBA was used. Only the rain events recorded during the time of an actively working pressure transducer were used in the analysis of a particular site.

For each site, all precipitation events were assigned a binary value for flow or no flow. Precipitation event metrics (Depth, I15, I30, I60) were then sorted from highest to lowest for each metric to determine which of the metrics best indicated precipitation thresholds for runoff production. A threshold was defined when the majority of the values above a given magnitude produced runoff, and the majority of values below that magnitude did not. Based on this analysis, the metric best suited for defining runoff thresholds was selected, and precipitation thresholds for runoff generation were compared between geomorphic groupings of channel types. The fraction of rain events producing runoff was also calculated by season and for the period of record, and compared between channel types.

5. RESULTS

5.1. Seasonality of rain

For this study, the year is broken-up into two seasons: winter (November - April) and summer (May - October). This division separates the convective systems that characterize warm-season precipitation from the frontal systems that supply cold season precipitation (Hallack-Alegria and Watkins, 2007). The seasonal patterns of precipitation are summarized in Table 5.1 and 5.2; data used for this analysis have some gaps due to data loss, and the values listed in the tables represent recorded values only. As mentioned in the Methods section, rain events when the rain gauge or pressure transducer were not working at a particular site have been removed from that site's data. Therefore this analysis does not try to surmise climate variations between sites and seasons. In this study area, most sites had more rain events and greater total rain depth recorded during the summer than during the winter months (Table 5.1). The average of all sites' total rain depth for the three winters was between 26-41 mm and between 43-114 mm for the two summers (Table 5.2). The range of winter rain event depths at all sites was between 1-31 mm, and the range of depth for the summer storms was from 1-87 mm (Table 5.2). The range of event depths during the summer was wider than the range during the winter, due to individual high depth summer storms. However, the average event depths for winter and summer were similar, with the summer averages ranging from 7-13 mm, and the winter averages ranging from 4-14 mm (Table 5.2). The winter of November 2011 - April 2012 was the driest winter, with an average site total depth of 26 mm and an average event depth of 4 mm (Table 5.2). The following summer, May 2012 - October 2012, was the wettest season during the study with an average site total depth of 114 mm and an average event depth of 13 mm (Table 5.2). Although there were more rain events and more rain accumulation in the summer, winters tended to have longer event durations. The average durations of the winter rain events were between 3.25-17 hours, whereas the average summer

rain events lasted 2.25-3.5 hours (Table 5.2). The range of winter storm duration was between 0.25 and 41.75 hours, and the range of summer rain duration was from 0.25 to 10.75 hours (Table 5.2). At most sites the total duration of rain during the summer was shorter than the winter (Table 5.1). YBK1 was the only site where the summer rain duration was longer than winter rain duration (Table 5.1). At most sites the average I60 of summer storms was greater than the average I60 of winter storms, ranging from 1.08 to 2.26 times greater (Table 5.1). YBK1 and YBA1 had average I60s of winter storms greater than summer storms. The average I60 of winter storms was 3-4 mm hr⁻¹, and summer storms average I60 was 5 and 11 mm hr⁻¹ (Table 5.2). The range of winter storms' I60 was between 1-24 mm hr⁻¹, and the range of summer I60s was up to 70 mm hr⁻¹ (Table 5.2).

Table 5.1: Seasonality of rain at each site, with differences between summer and winter total recorded precipitation depth, total duration, and storm average I60 for Nov 2012 – Oct 2013. YPH1 is not included because the majority of the PT data between 9/23/2012 – 12/6/13 was not usable. YBK2, MBK2, MBA2, and YIA2 are not included because they were installed in February or March of 2013.

Site	Number of winter rain events	Number of summer rain events	Depth during year (mm)	% total depth occurred in winter	% of total depth occurred in summer	Duration ratio Summer/Winter	Average I60 ratio Summer/Winter
Piedmont Headwaters							
MPH1	5	3	81	63.4	36.6	0.26	2.26
Bedrock							
YBK1	3	10	61	38.8	61.2	2.80	0.48
Bedrock with Alluvium							
YBA1	5	10	87	56.7	43.3	0.93	0.55
MBA1	4	9	157	35.3	64.7	0.98	1.53
Incised Alluvium							
YIA1	5	8	87	49.7	50.3	0.80	1.09
Braided							
MIA1	4	5	91	59.4	40.6	0.57	1.12
YBD1	3	7	98	44.7	55.3	0.94	1.08
MBD1	5	3	81	63.4	36.6	0.26	2.26

Table 5.2: Seasonality of rain for sites with continuous measurements during three winters (Nov-Apr) and two summers (May-Oct). Sites used: YPH1, MPH1, YBK1, YBA1, MBA1, YIA1, MIA1, YBD1, and MBD1.

	Average total depth (mm)	Average event depth (mm)	Range of event depth (mm)	Average total duration (hrs)	Average event duration (hrs)	Range of event duration (hrs)	Average event I60 (mm hr ⁻¹)	Range of event I60 (mm hr ⁻¹)
Winter								
Winter 11-12	26	4	1 - 24	19	3.25	0.25 - 15.5	3	1 - 24
Winter 12-13	41	11	1 - 25	27.25	7.25	0.5 - 20.75	4	1 - 12
Winter 13-14	27	14	1 - 31	34	17	0.5 - 41.75	3	1 - 6
Summer								
Summer 12	114	13	1 - 87	20.25	2.25	0.25 - 12	11	1 - 70
Summer 13	43	7	1 - 53	21.25	3.5	0.25 - 10.75	5	0 - 28

5.2. Rainfall-runoff events

The sites experienced between 11 and 48 rain events from November 2011 to May 2014 that caused between 0 to 9 runoff events (Table 5.3). Most of the runoff-producing rain events affected the entire study area, though the storm total depth and maximum intensity varied across the watersheds (Figure 5.1-5.2). Because of this variance, most of the flows were localized to only one or two sites. Only the storm on 7/13/12 had flow recorded throughout both watersheds (Figure 5.3). With the exception of 11 runoff-producing storms of 9 hours or more, most runoff-producing storm event durations were between 1 and 4 hours.

The 7/13/12 event was the largest runoff event recorded in both watersheds during this study (Figure 5.3). The storm that produced this runoff generally had the most rain and highest I60 (Figure 5.1-5.2). The I60 of most sites fell in the range of 63-70 mm hr⁻¹, with the highest intensity of 70 mm hr⁻¹ recorded at YBK1 (Figure 5.1). Most sites received between 64-87 mm of rain (Figure 5.2). The lowest recorded I60 and depth for this event was at MBD1, which was 9 mm hr⁻¹ and 18 mm.

Table 5.3: Time period analyzed for each site, total precipitation measured at the site, and total number of rainfall and runoff events by site.

Site Name	Start date	Last download	Total Precip (mm)	Total rain events	Total runoff events	% rain causing runoff
Piedmont Headwaters						
YPH1	3/14/2012	5/12/2014	151	11	4	36
MPH1	11/12/2011	5/11/2014	231	29	9	31
Bedrock						
YBK1	11/12/2011	5/12/2014	276	30	7	23
YBK2	3/20/2013	5/13/2014	83	12	2	17
MBK2	2/9/2013	5/15/2014	80	12	3	25
Bedrock with Alluvium						
YBA1	11/13/2011	5/12/2014	310	31	3	10
MBA1	11/13/2011	5/11/2014	299	22	2	9
MBA2	2/9/2013	5/15/2014	80	12	0	0
Incised Alluvium						
YIA1	11/13/2011	5/12/2014	255	25	5	20
YIA2	3/20/2013	5/13/2014	74	11	0	0
Braided						
MIA1	11/13/2011	5/14/2014	325	48	2	4
YBD1	2/17/2012	5/13/2014	206	19	1	5
MBD1	4/1/2012	5/14/2014	205	26	1	4

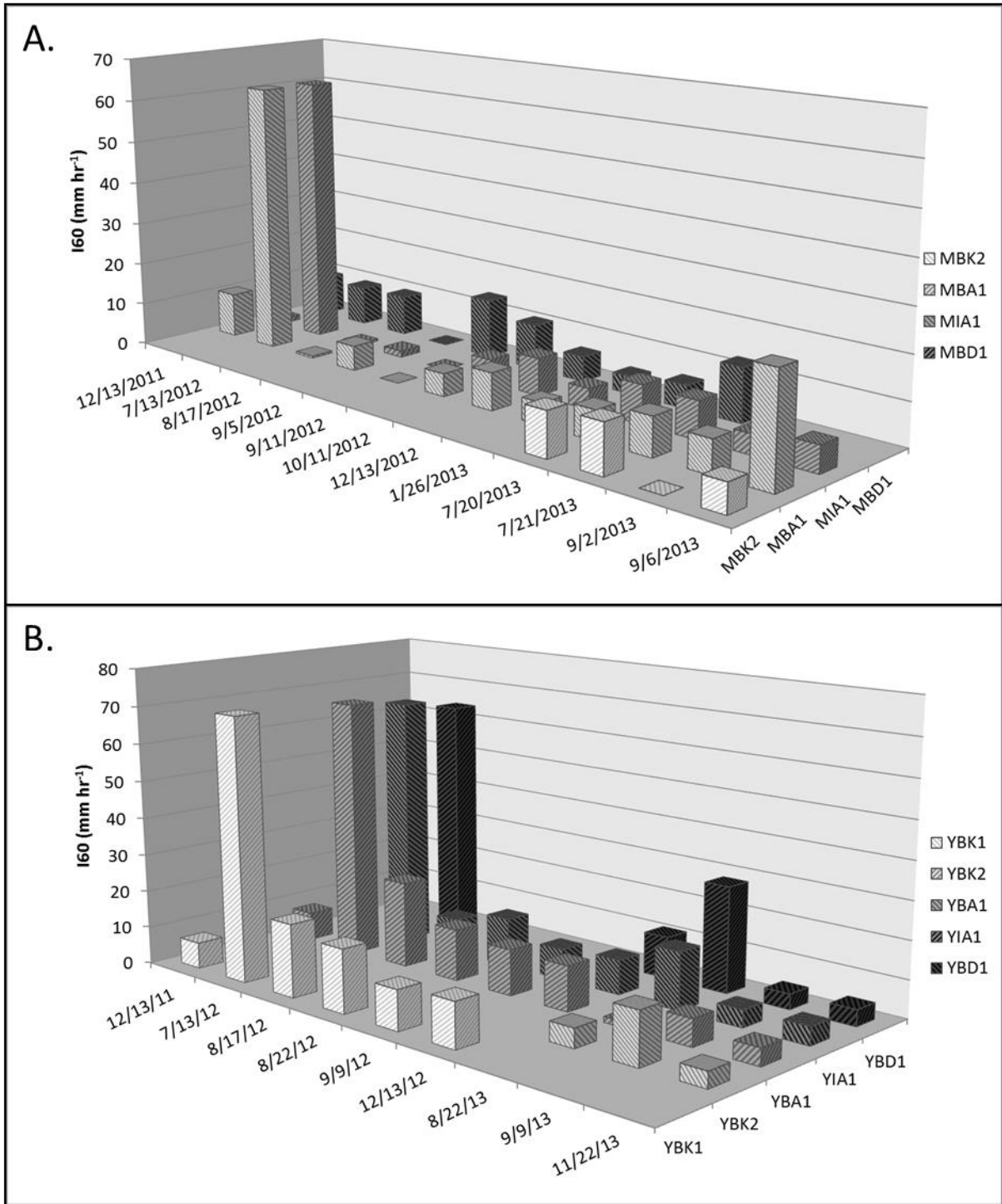


Figure 5.1. Spatial variability of peak I60 for rain events that produced runoff at one or more monitoring locations. Times of no rain are illustrated by flat boxes, and no boxes indicate equipment was not recording during this time. (A) rain gauges in Mohave Wash, (B) rain gauges in Yuma Wash.

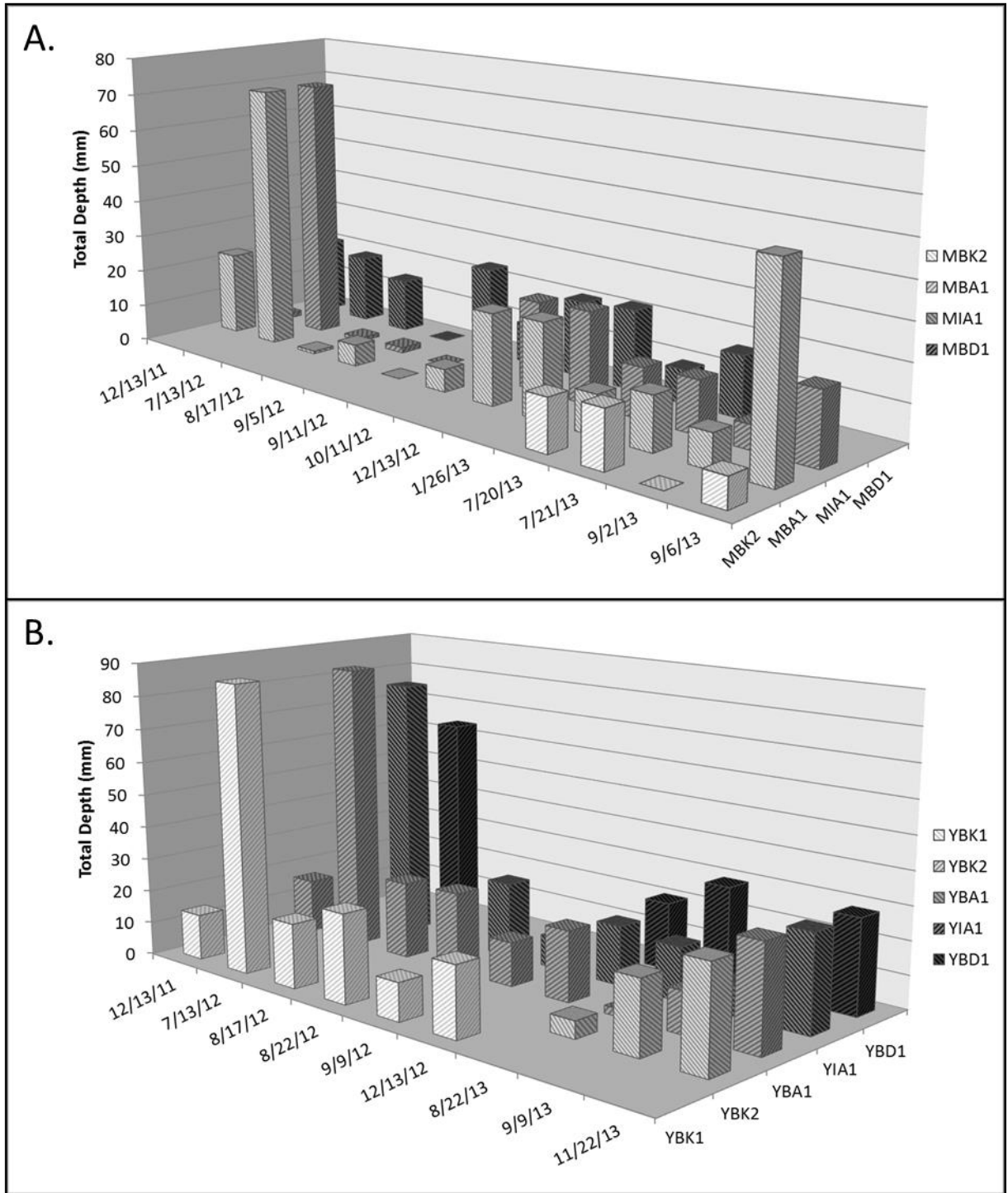


Figure 5.2. Spatial variability of total storm depth for rain events that produced runoff at one or more monitoring locations. Times of no rain are illustrated by flat boxes, and no boxes indicate equipment was not recording during this time. (A) rain gauges in Mohave Wash, (B) rain gauges in Yuma Wash.

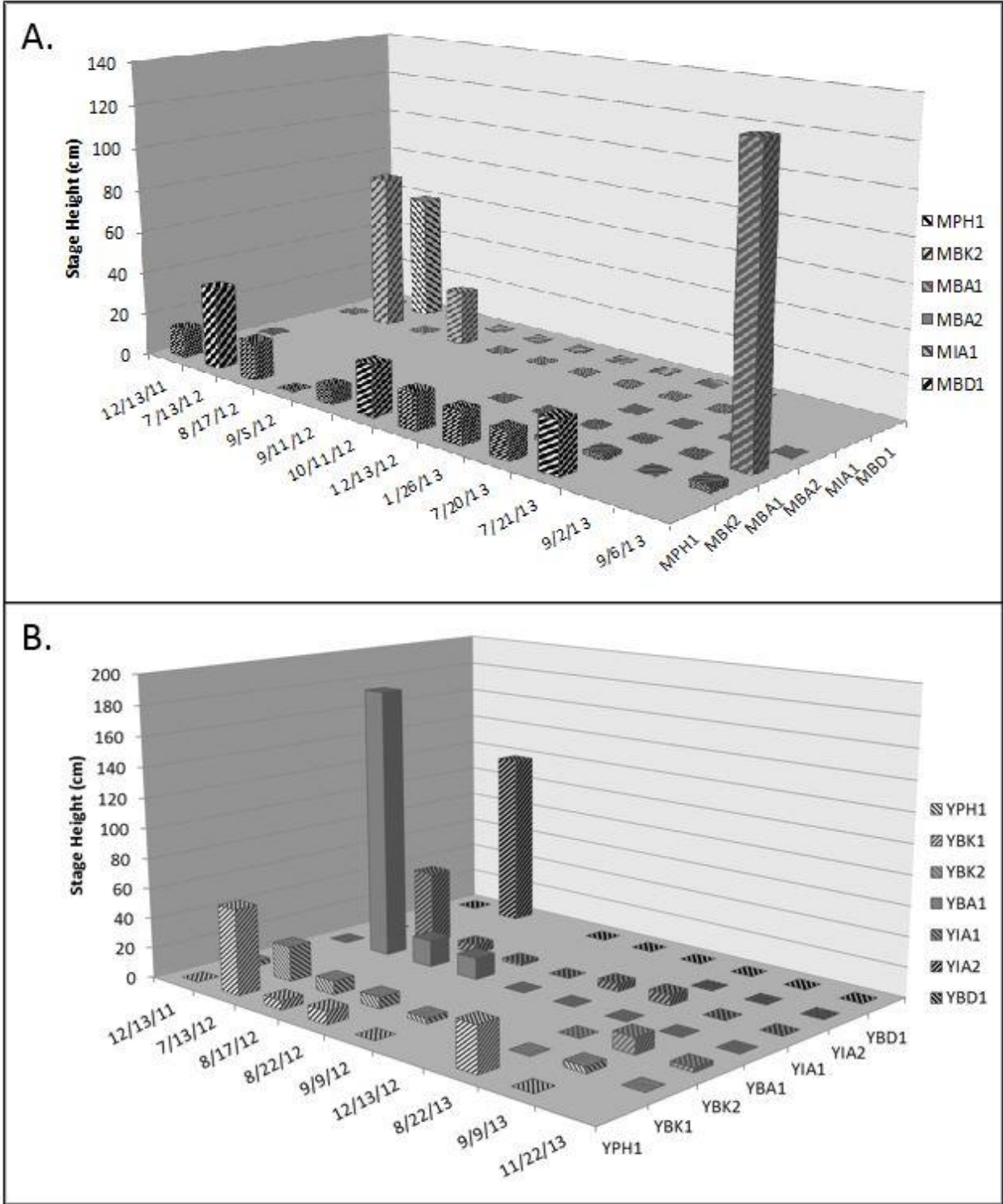


Figure 5.3. Spatial variability of flow occurrence for rain events that produced runoff at one or more monitoring locations. Times of no flow are illustrated by flat boxes, and no boxes indicate equipment was not recording during this time. (A) pressure transducers in Mohave Wash, (B) pressure transducers in Yuma Wash.

Runoff was recorded at all of the sites that were operational during the 7/13/12 rain event. The pressure transducer at MBA1 was washed away and lost during this flow, so although no stage data were recorded there, flow occurrence at MBA1 during this event was used in the threshold analysis. Peak stage heights at the remaining sites ranged from 23 cm at YBK1 up to 180 cm at YBA1 (Figure 5.3-5.4). In Yuma Wash the flow started at YBK1 (Figure 5.4). The flow pulse then traveled down to YBA1, where it had the highest peak stage, then to YIA1 further downstream, and finally to the furthest downstream site, YBD1, where the flow continued for 4.5 hours and peaked at 118 cm (Figure 5.4). In this watershed, high rain throughout the watershed led to the sustained flow at the braided channel location farthest downstream. In Mohave Wash flow was first recorded at MPH1, which then peaked again due to a second rainfall over 3 hours later. The main flow pulse was first recorded at MIA1 just over two hours before it reached MBD1. In contrast to Yuma Wash, where flow duration was longest at the braided site, MIA1 had the longest flow duration of 6.25 hours, and MBD1 had the shortest of 1 hour with a quickly rising and falling hydrograph peaking at 60cm (Figure 5.4). In Mohave Wash, the rain storm was not as large in the lower watershed near the braided site; the high sustained flow at the MIA1 site upstream was recorded in a confined stretch of channel, which widens downstream into a braided channel. Much of the flow at MIA1 must have been lost to channel transmission before reaching the MBD1 site.

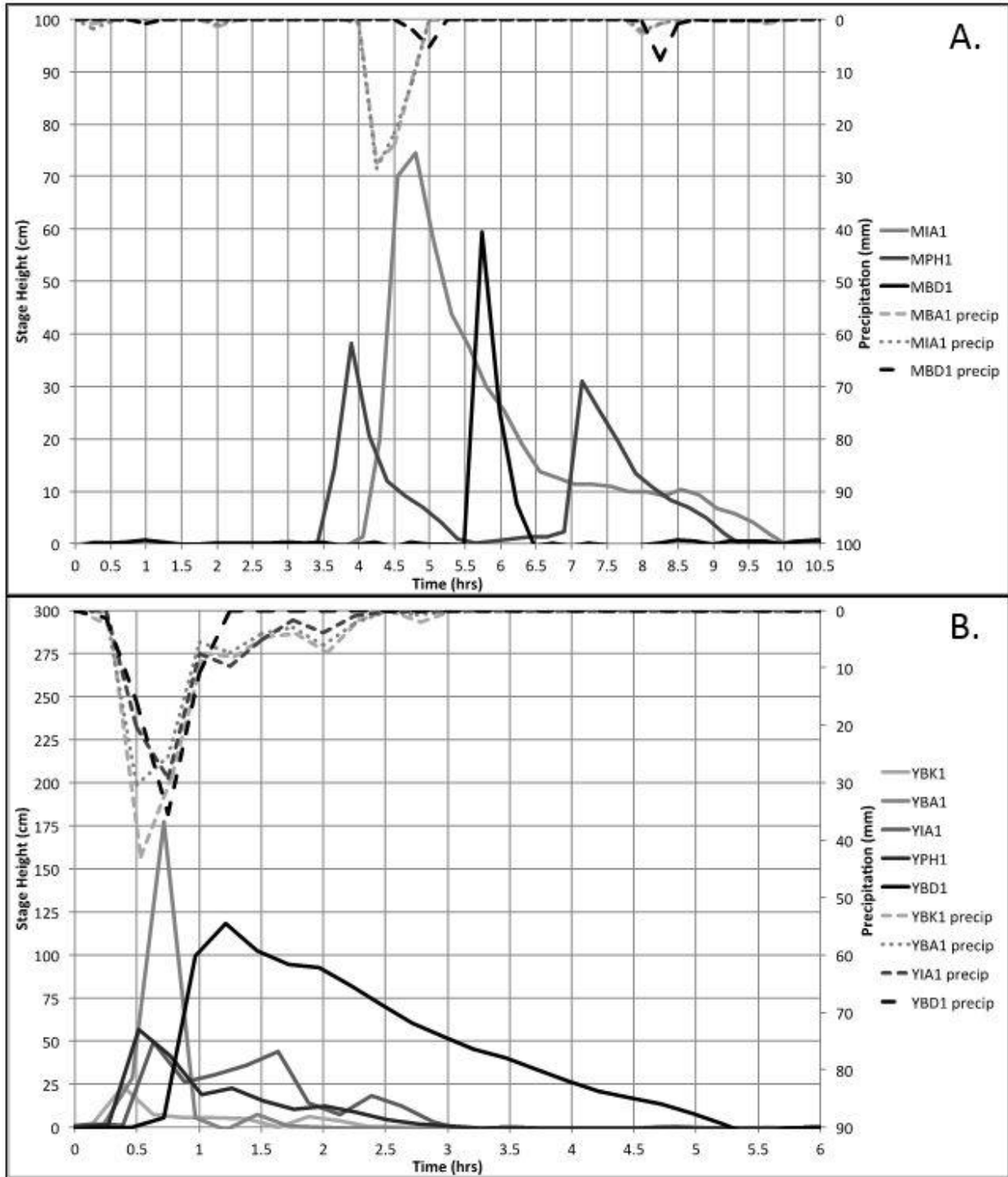


Figure 5.4. Hydrographs of the 7/13/12 flow event at both watersheds. Sites in the order of upstream to downstream. (A) Mohave Wash, (B) Yuma Wash.

Only four sites recorded flow during the winter: MPH1, YBK1, YBK2, and YIA1 (Table 5.4). With the exception of the one winter flow at YIA1, all of these sites with winter flows were at the small

bedrock and piedmont headwater catchments. MPH1 experienced the most runoff-producing rains (9; Table 5.3), and the most winter flows (3; Table 5.4). YIA1 had 20 percent of runoff producing rains occurring in winter, which was the lowest percentage out of the sites that experienced winter runoff. Fifty percent of the runoff at YBK2 occurred during winter, but there were only two flows, one in summer and one in winter (Table 5.4).

Table 5.4: Seasonality of runoff-producing rain events.

Site Name	Winter rain events that caused flow	Summer rain events that caused flow	% runoff producing rains that occurred during winter	% runoff producing rains that occurred during summer
Piedmont Headwaters				
YPH1	0	4	0	100
MPH1	3	6	33	67
Bedrock				
YBK1	2	5	29	71
YBK2	1	1	50	50
MBK2	0	3	0	100
Bedrock with Alluvium				
YBA1	0	3	0	100
MBA1	0	2	0	100
MBA2	0	0	0	0
Incised Alluvium				
YIA1	1	4	20	80
YIA2	0	0	0	0
Braided				
MIA1	0	2	0	100
YBD1	0	1	0	100
MBD1	0	1	0	100

Table 5.5 summarizes the lag time between the peak of a runoff-producing rain event and the peak of the runoff event. In some cases the peak flow occurred at the monitoring site before the rain gauge measured the peak rain. This is shown in Table 5.5 as negative lag times. The average lag times at each site were less than half an hour, and with the exception of two events, the lag times for individual events were less than an hour (Table 5.5). The piedmont headwater sites have the greatest distances

between pressure transducers and rain gauges and have the largest range of lag times (Table 5.5).

Excluding incised alluvium and braided sites, flow-monitoring sites with rain gauges on site had small ranges in lag times, no greater than half an hour (Table 5.5). The one flow event at MBD1 had a lag time of -2.5 hours, which reflects flow responding to precipitation upstream in the watershed, before peak precipitation at the MBD1 site.

Table 5.5: Summary statistics for rainfall-runoff event timing. Lag times for runoff events are expressed as lag time between peak 15-minute precipitation and peak 15-minute stream stage. Positive values of lag time indicate precipitation peaked before stream stage; negative values indicate stream stage peaked before precipitation.

Site	Distance to rain gauge (km)	Average flow duration (hrs)	Range of flow duration (hrs)	Average rain duration (hrs)	Range of rain duration (hrs)	Average lag time (hrs)	Range of lag times (hrs)	Average peak stage (cm)	Range of peak stage (cm)
Piedmont Headwaters									
YPH1	1.0	1.25	0.5 to 3	2.25	1 to 3.25	0.25	0 to 0.75	25	6 to 57
MPH1	1.5	3.50	2.25 to 4.75	7.50	2 to 18.25	-0.50	-0.25 to -1.25	15	0.3 to 23
Bedrock									
YBK1	0.3	1.00	0.5 to 2.25	4.75	1.25 to 13	0.25	0 - 0.5	8	4 to 23
YBK2	0.0	0.75	0.5 to 0.75	19.25	10.25 to 28.25	0.50	0.25 to 0.5	7	3 to 11
MBK2	0.0	2.00	1.5 to 2.5	4.00	3.25 to 4.25	0.00	0 to 0.25	2	2 to 3
Bedrock with Alluvium									
YBA1	0.0	1.25	0.5 to 2.0	2.50	1.25 to 3	0.25	0 to 0.5	71	14 to 181
MBA1	0.0	34.75	30 to 45	7.25	4.5 to 10	0.00	0 to 0.25	133	133
MBA2	1.3	No Flow							
Incised Alluvium									
YIA1	0.0	2.25	0.25 to 4.25	3.00	1 to 6	0.25	0 to 0.75	14	2 to 49
YIA2	1.4	No Flow							
Braided									
MIA1	0.0	4.00	1.5 to 6.5	6.25	0.5 to 12	0.75	0.25 to 0.75	50	25 to 75
YBD1	0.0	4.75	4.75 to 5.0	1.00	1 to 1.25	0.50	0.25 to 0.5	118	118
MBD1	0.0	1.25	1 to 1.25	9.00	9 to 9.15	-2.50	-2.5 to -2.75	60	60

5.3. Selection of rain event metrics for threshold analysis

Table 5.6 compares the four precipitation metrics (Depth, I15, I30, I60) at each site to identify how well the metric did at sorting flow-producing rain events above a threshold. For each metric the number of no-flow rain events over the threshold (false positive) and the number of flow-producing rain

events under the threshold (false negative) out of the total number of flows were identified. The metrics that had the lowest total number of false positives and false negatives were then identified and noted in the final column (Table 5.6).

Table 5.6: Comparison of storm depth, 15-minute, 30-minute, and 60-minute peak intensities for predicting runoff thresholds for each site. FP (false positive) is no-flow rain events above the threshold, and FN (false negatives) is flow-producing rain events below the threshold. The best metrics for each site are those with the lowest total number of FP+FN.

Site	# rain events	Total depth		15 min		30 min		60 min		Best	
		FP	FN	FP	FN	FP	FN	FP	FN		% correctly identified
Piedmont Headwaters											
YPH1	11	1	0	1	0	1	0	0	0	60	100
MPH1	29	1	0	0	3	1	1	1	1	Depth	97
Bedrock											
YBK1	30	1	0	1	0	0	0	0	0	30, 60	100
YBK2	12	0	0	3	0	2	0	1	0	Depth	100
MBK2	12	1	0	0	0	0	0	0	0	15, 30, 60	100
Bedrock with Alluvium											
YBA1	31	1	0	1	0	0	0	0	0	30, 60	100
MBA1	22	0	0	0	0	0	0	0	0	Depth, 15, 30, 60	100
MBA2	12	No Flow	No Flow	No Flow	No Flow	No Flow	No Flow	No Flow	No Flow		No Flow
Incised Alluvium											
YIA1	25	2	1	1	0	1	0	0	0	60	100
YIA2	11	No Flow	No Flow	No Flow	No Flow	No Flow	No Flow	No Flow	No Flow		No Flow
Braided											
MIA1	48	0	1	0	1	0	1	0	1	Depth, 15, 30, 60	98
YBD1	19	0	0	0	0	0	0	0	0	Depth, 15, 30, 60	100
MBD1	26	4	0	1	0	2	0	4	0	15	96

Table 5.7 compares how the four metrics did at organizing the runoff producing events above a threshold. The overall percent accuracy is calculated as:

$$\frac{E - FP - FN}{E} \times 100$$

where E is the total number of rain events. I60 was found to produce the best indication of a precipitation threshold for runoff, with precipitation events sorted with decreasing I60s having the majority of corresponding flow events at the top of the list. The I60 metric was one of the best-performing threshold metrics for 8 out of the 11 sites with 97.2% overall accuracy (Table 5.7). The I30

metric was the next best with an accuracy of 96.9%, followed by I15 with an accuracy of 95.8%, and then depth with an accuracy of 95.5% (Table 5.7). All four metrics could be used to create thresholds for the different sites with an accuracy of 95.5% and greater. I60 had an overall percent accuracy only 1.7% greater than the worst metric, but it predicted 7 sites with 100% accuracy, whereas the other metrics only predicted 3 to 5 sites with 100% accuracy (Table 5.6). Because I60 was overall the best metric for identifying runoff thresholds, this metric was used in subsequent threshold analysis.

Table 5.7: Summary of site-based threshold analysis in Table 5.6, indicating the number of sites for which each metric was or was not among the best metrics for identifying runoff thresholds.

Metric	Overall % accuracy	# of sites metric was among the best choices	# of sites metric was not among the best choices
Depth	95.5	5	6
I15	95.8	5	6
I30	96.9	6	5
I60	97.2	8	3

5.4. Runoff thresholds by channel type

The precipitation thresholds for runoff generation varied between channel types. Pressure transducers at two Piedmont Headwater sites, YPH1 and MPH1, were used in the threshold analysis for piedmont headwater channels. Table 5.8 and Figure 5.5 shows the total depth and I60 threshold range and mean for each site. Precipitation values are reported to the nearest 0.1 mm to illustrate differences, but the precision of the rain gauges is 0.25 mm per tip. The lower end of the threshold range is the highest total storm depth and I60 that did not produce runoff, excluding false negatives, and the upper end of the threshold range is the lowest total storm depth and I60 that created runoff, excluding false positives. The mean of the threshold range in Table 5.8 is the mean of the lower and upper threshold limits. Figure 5.6 shows I60 plotted against the total storm depth for the rain gauges at MBD1 and YIA1 with the corresponding flow events at MPH1 and YPH1.

The range of the total depth threshold at YPH1 was between 4.8-8.9 mm (Table 5.8, Figure 5.6). This gave a mean total depth threshold of 6.9 mm at YPH1. YPH1 had an I60 threshold range of 8.1-8.9 mm hr⁻¹, which gave it a mean threshold of 8.5 mm hr⁻¹ (Table 5.8 and Figure 5.5, 5.5). There were no false positives or false negatives for YPH1's I60 threshold. MPH1 had a total depth threshold range between 5.8-8.9 mm, with a threshold mean of 7.4 mm. The I60 threshold for MPH1 was between 4.6-5.3 mm hr⁻¹. The mean of this threshold range was 5.0 mm hr⁻¹. Rain events around the I60 threshold at YPH1 have a recurrence interval of one year, and at MPH1 the recurrence interval for the threshold is less than one year (Bonnin et al., 2011).

At MPH1 there was one rain event over the I60 threshold that did not produce flow, and one high magnitude winter rain event that produced runoff under the I60 threshold (Figure 5.6). This winter event occurred on January 26, 2013 and had a high total depth of 21 mm and an I60 of 4 mm hr⁻¹ (Figure 5.1-5.2). The total depth metric worked the best at defining a runoff threshold at this site (Table 5.6). The storm total depth threshold separates flow and no flow events independent of storm intensity.

Table 5.8: Depth and I60 precipitation thresholds by site. ‘Below threshold’ indicates the highest value of the precipitation metric (depth or I60) with no flow, excluding FN, and ‘above threshold’ indicates the lowest value of the precipitation metric with flow, excluding FP. Mean threshold values are the mean of the precipitation values below and above the threshold.

Site Name	Depth below threshold (mm)	Depth above threshold (mm)	Mean of depth threshold range (mm)	I60 below threshold (mm hr ⁻¹)	I60 above threshold (mm hr ⁻¹)	Mean of threshold I60 range (mm hr ⁻¹)
Piedmont Headwaters						
YPH1	4.8	8.9	6.9	8.1	8.9	8.5
MPH1	5.8	8.9	7.4	4.6	5.3	5.0
Bedrock						
YBK1	7.9	11.4	9.6	4.6	7.0	5.8
YBK2	7.8	21.8	14.8	3.9	4.2	4.0
MBK2	4.8	7.8	6.3	6.1	6.6	6.4
Bedrock Alluvium						
YBA1	21.1	23.1	22.1	12.2	13.7	13.0
MBA1	31.0	52.6	41.8	10.4	25.2	17.8
MBA2	24.6	no flow	no flow	11.3	no flow	no flow
Incised Alluvium						
YIA1	9.4	16.0	12.7	8.1	8.9	8.5
YIA2	29.0	no flow	no flow	15.2	no flow	no flow
Braided						
MIA1	30.7	70.9	50.8	23.9	62.7	43.3
YBD1	29.2	63.8	46.5	28.2	63.8	46.0
MBD1	16.3	18.3	17.3	5.8	9.1	7.5

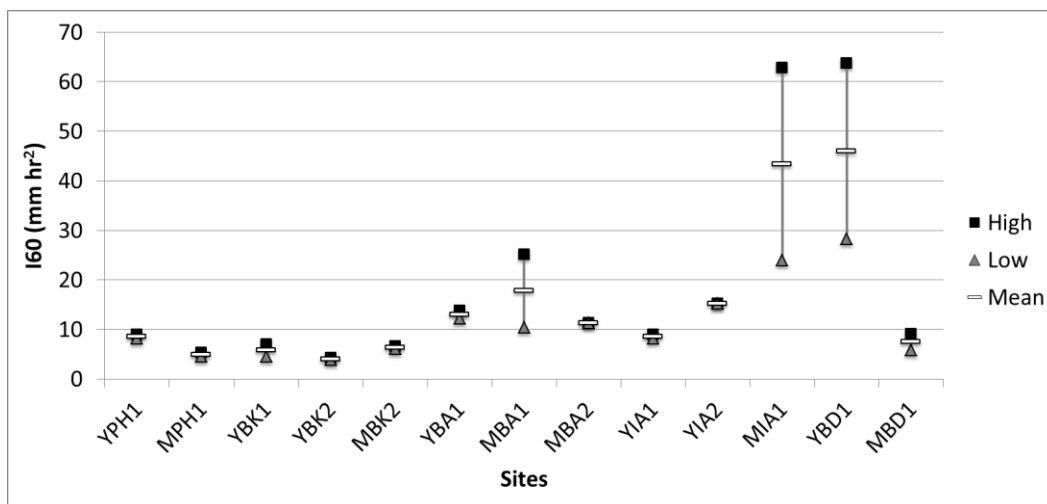


Figure 5.5. Range of I60 thresholds by site. For each site the low value is the highest I60 that did not produce runoff, excluding FN, and the high value is the lowest I60 that produced runoff, excluding FP.

The mean of the upper and lower ends of the threshold is shown as a horizontal line. MBA2 and YIA2 did not have flow, so the mean horizontal line is the highest I60 recorded at that site. Data in Table 5.8.

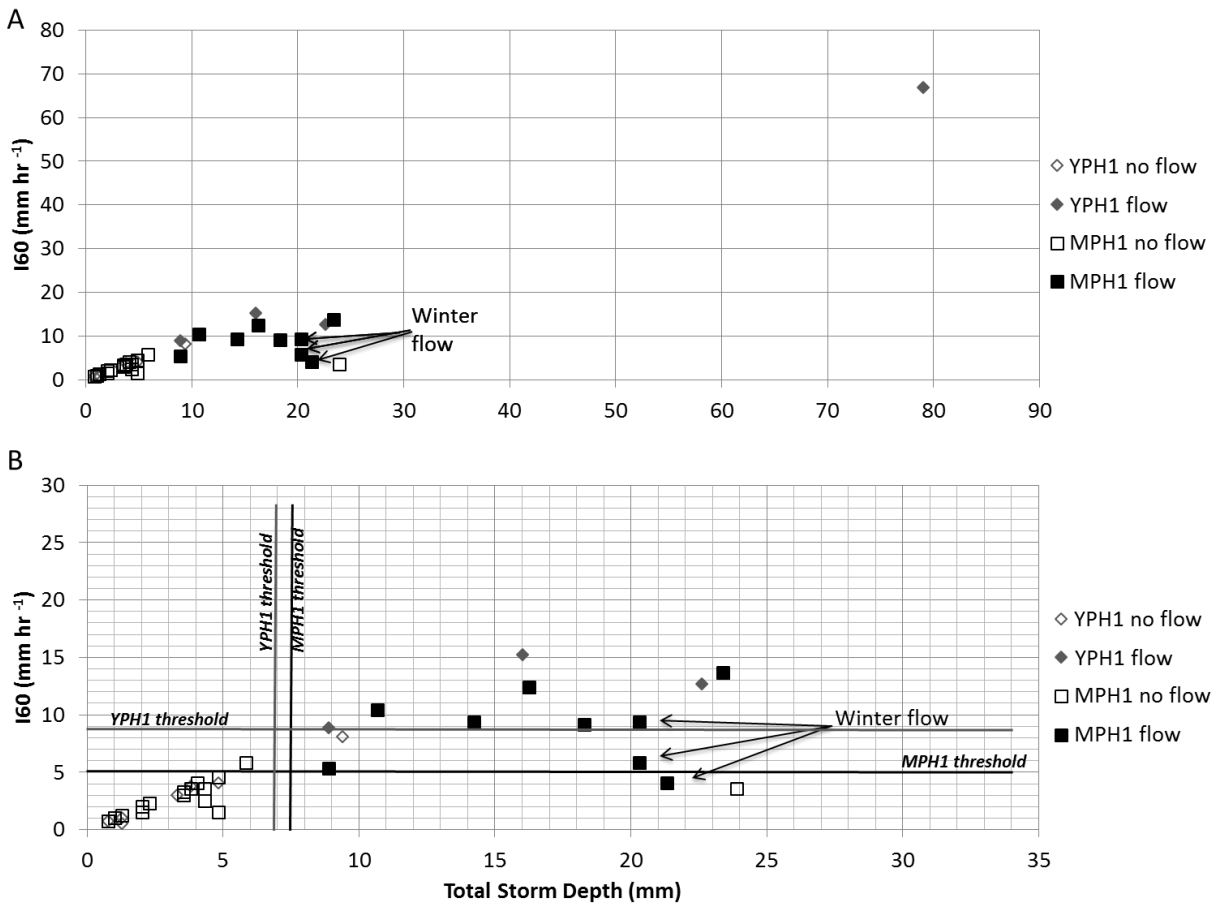


Figure 5.6. Piedmont Headwaters I60 vs total storm depth of all storm events. Diamonds represent rain events at YPH1, and squares represent MPH1. Open symbols represent rain events that did not produce runoff, and solid symbols represent rain events that produced runoff at that site. (A) all rain events and (B) close-up around threshold.

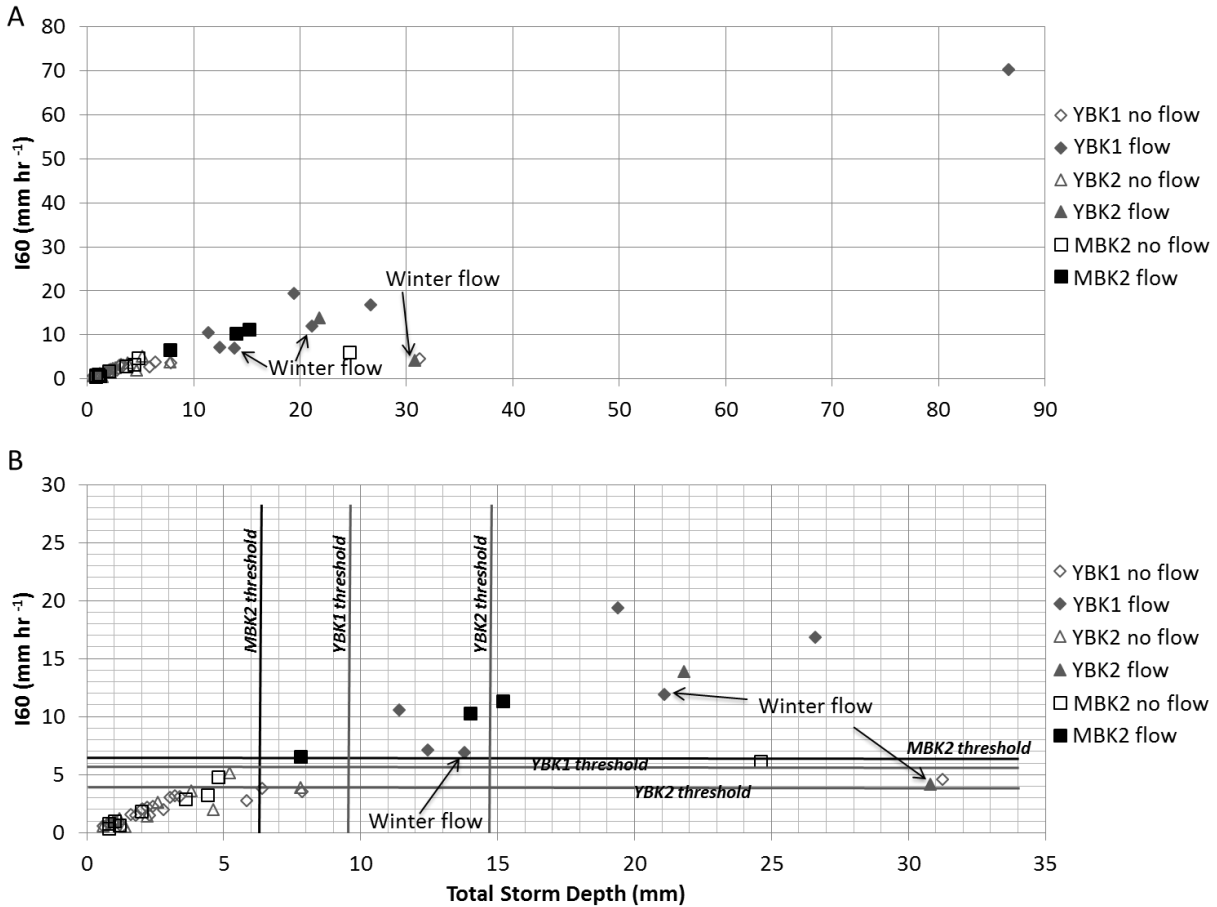


Figure 5.7. Bedrock channels I60 vs total storm depth of all storm events. Diamonds represent rain events at YBK1, triangles represent YBK2, and squares represent MBK2. Open symbols represent rain events that did not produce runoff, and solid symbols represent rain events that produced runoff at that site. (A) all rain events and (B) close-up around threshold.

The bedrock channel types had thresholds in a similar range as those in the piedmont headwater sites. Figure 5.7 shows the precipitation events at the bedrock channels and whether or not there was flow associated with the event. YBK1 had a rain gauge on site until February 10, 2013; after this date the rain data came from YBA1, which is 0.3 km away (Table 4.1). YBK's threshold range for total depth was between 7.9-11.4 mm, which gave it a mean threshold of 9.6 mm (Table 5.8). YBK1 showed a clear runoff-producing I60 threshold between the highest I60 rain event that did not produce runoff, with an I60 of 4.6 mm hr⁻¹, and the lowest I60 rain event that did produce runoff, with an I60 of 7.0 mm hr⁻¹ (Figure 5.7). This gave an estimated I60 threshold of 5.8 mm hr⁻¹ (Table 5.8). There were no no-flow

rain events above this threshold, and no flow events below it. YBK2 had a total depth range between 7.8-21.8 mm. This was a large range, and the mean threshold of 14.8 mm was higher than the other sites. YBK2 had an I60 threshold range of 3.9-4.2 mm hr⁻¹ (Table 5.8, Figure 5.5). This gave an estimated I60 threshold of 4.0 mm hr⁻¹. There was one no-flow rain event above this threshold. MBK2's total depth threshold range was between 4.8-7.8 mm with a mean of 6.3 mm. The MBK2 site's range for the I60 runoff producing threshold was from 6.1-6.6 mm hr⁻¹, and had an estimated threshold of 6.4 mm hr⁻¹. No flows occurred under this threshold, and no no-flow rain events occurred above it (Table 5.8 and Figure 5.7). The estimated I60 thresholds at YBK1, YBK2, and MBK2 have a recurrence interval of less than one year (Bonnin et al., 2011).

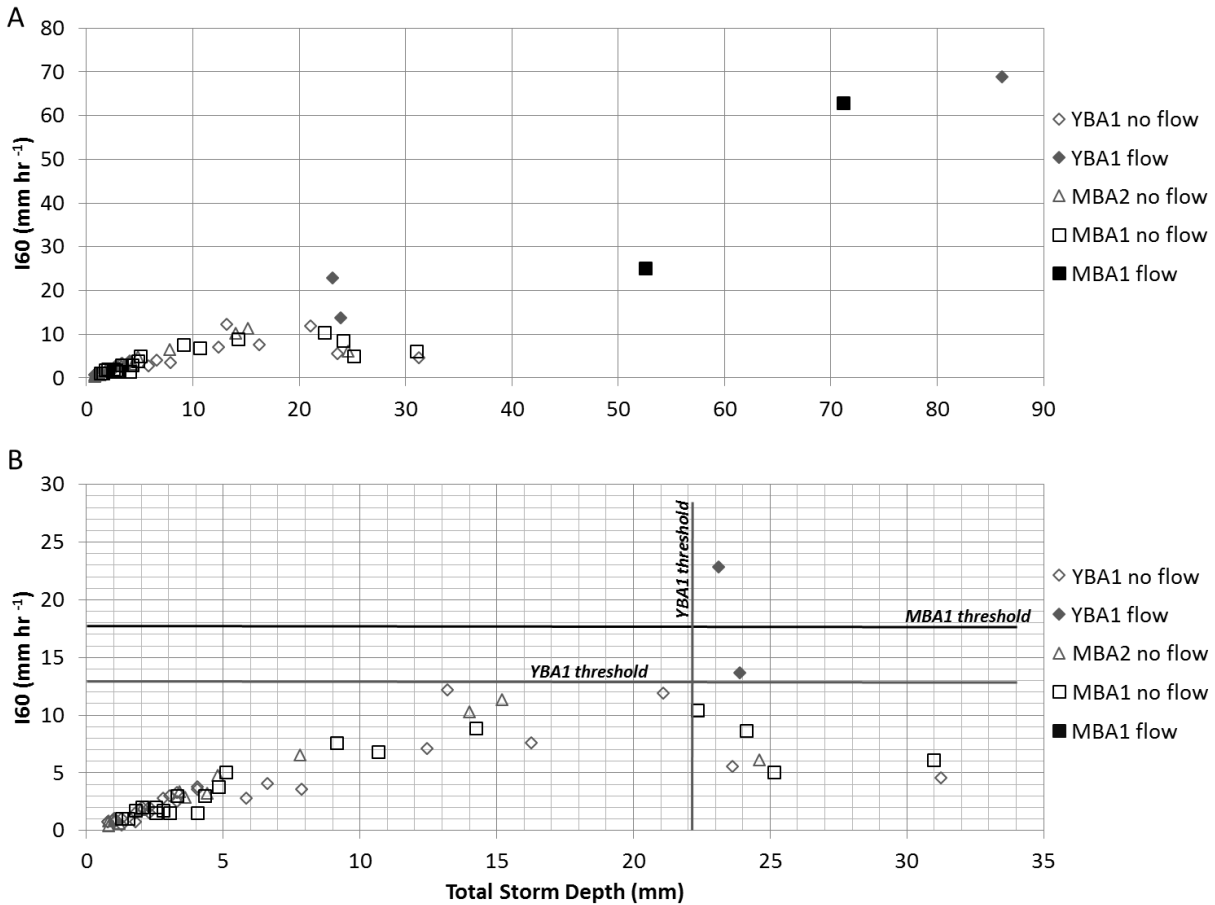


Figure 5.8. Bedrock with Alluvium channel I60 vs total storm depth of all storm events. Diamonds represent rain events at YBA1, triangles represent MBA2, and squares represent MBA1. Open symbols represent rain events that did not produce runoff, and solid symbols represent rain events that produced runoff at that site. (A) all rain events and (B) close-up around threshold.

Bedrock with alluvium channel types had larger precipitation thresholds than the PH and BK channel types. The range of the total depth threshold at YBA1 was between the total depth of the largest no-flow producing rain event below the threshold, which is 21.1 mm, and the smallest total depth of the runoff producing rain event directly above the threshold of 23.1 mm (Table 5.8 and Figure 5.8). This gave a mean total depth threshold of 22.1 mm at YBA1. The YBA1 site had an I60 runoff-producing threshold between 12.2-13.7 mm hr⁻¹ (Table 5.8 and Figure 5.5, 5.7). This produced an estimated threshold around 13.0 mm hr⁻¹, with no rain events producing runoff below it and no no-flow rain events above it. MBA1 had a total depth threshold ranging between 31.0-52.6 mm, with a mean

threshold of 41.8 mm. The I60 runoff-producing threshold at MBA1 was between 10.4-25.2 mm hr⁻¹ (Table 5.8 and Figure 5.5, 5.7). This was a large range, with the average between these rain events at 17.8 mm hr⁻¹, which correctly predicted no-flow and flow rain events. MBA2 did not have flow during the time of its operation. The highest total depth recorded during a rain event was 24.6 mm, and the most intense rain event recorded at MBA2 had an I60 of 11.3 mm hr⁻¹. The highest I60 rain event is shown as the lower end of the threshold in Figure 5.5. The recurrence interval for the estimated I60 threshold at YBA1 is 2 years, and between 2 and 5 years for the estimated I60 threshold at MBA1.

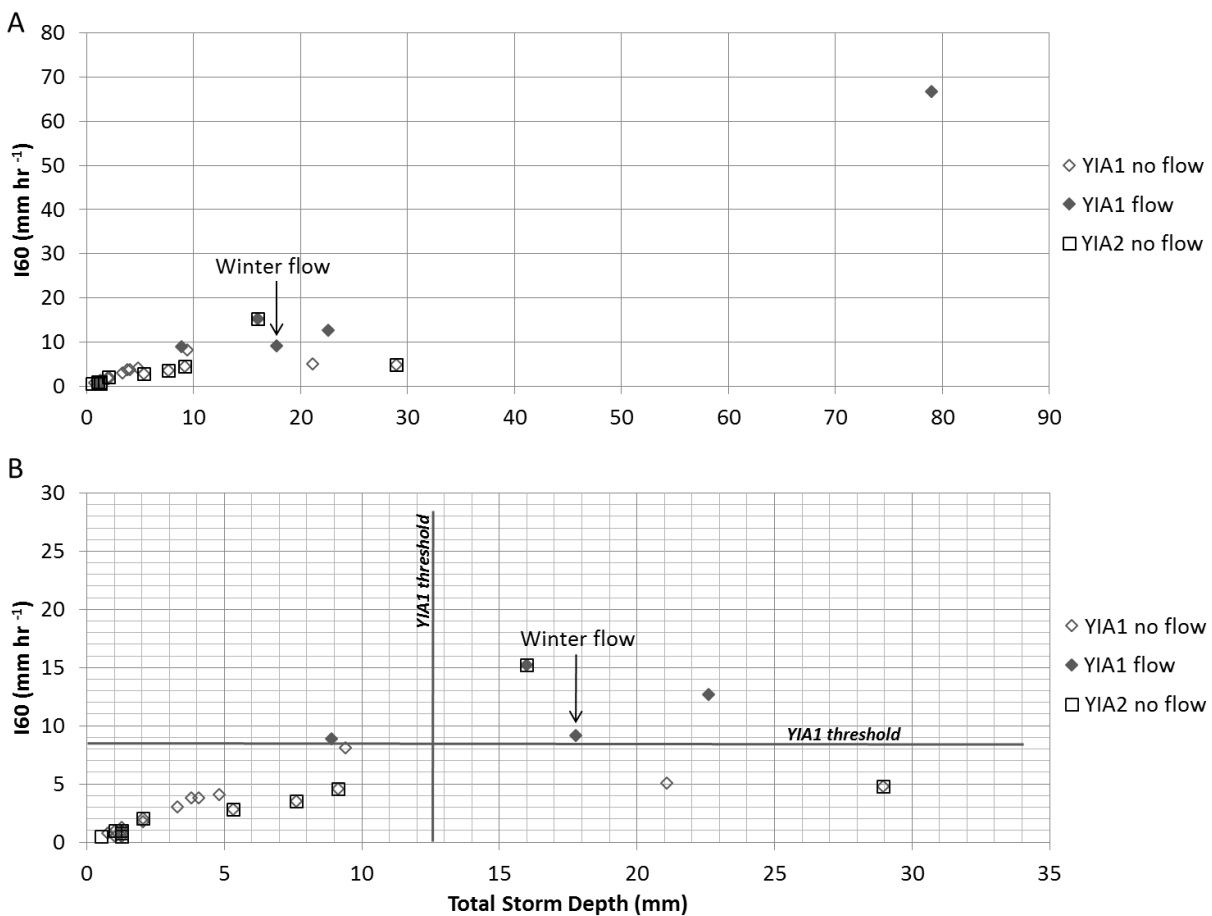


Figure 5.9. Incised Alluvium channels I60 vs total storm depth of all storm events. Diamonds represent rain events at YIA1 and squares represent YIA2. Open symbols represent rain events that did not produce runoff, and solid symbols represent rain events that produced runoff at that site. (A) all rain events and (B) close-up around threshold.

Data for threshold analysis at incised alluvium channel types were more limited, with only one site producing flow. At this site, YIA1, the mean of the runoff producing, total depth threshold was 12.7 mm, and the range was between 9.4-16.0 mm (Table 5.8 and Figure 5.9). The highest I60 of a no-flow producing rain event at YIA1 was 8.1 mm hr⁻¹, and the lowest I60 of a runoff producing rain event was 8.9 mm hr⁻¹, so the I60 runoff threshold at this site was estimated to be 8.5 mm hr⁻¹ (Table 5.8 and Figure 5.5). This threshold accounts for all no-flow and flow events. This was the same threshold range as listed for YPH1, which used the YIA1 rain gauge in the threshold analysis.

YIA2 did not record flow. The largest total storm depth recorded was 29.0 mm, and the highest I60 recorded during a rain event was 15.2 mm hr⁻¹, which has a 2-year recurrence interval (Table 5.8). Both values were above the depth and I60 thresholds that would have produced flow at YIA1, so YIA2's threshold was different than that of YIA1. Figure 5.5 only shows the lower end of the threshold range for YIA2.

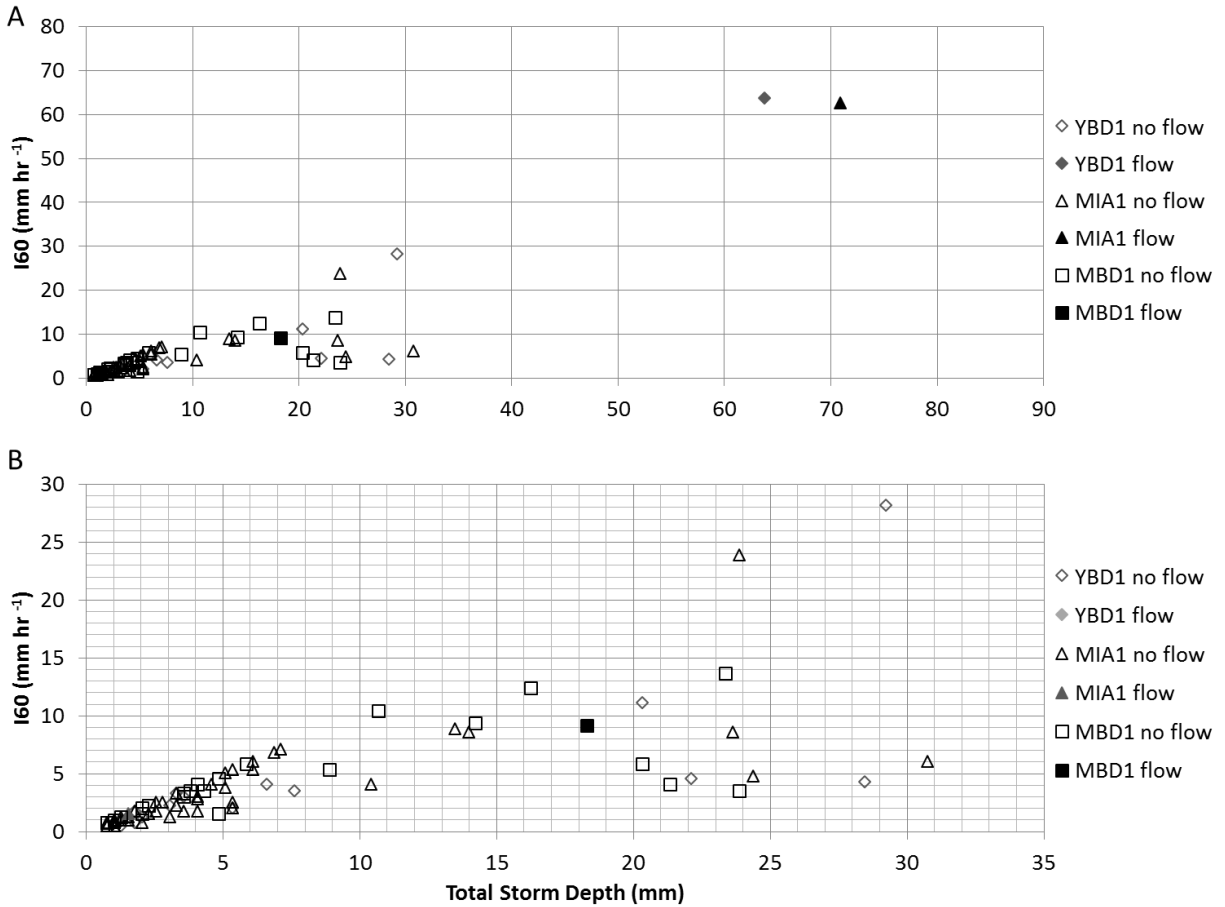


Figure 5.10. Braided channels I60 vs total storm depth of all storm events. Diamonds represent rain events at YBD1, triangles represent MIA1, and squares represent MBD1. Open symbols represent rain events that did not produce runoff, and solid symbols represent rain events that produced runoff at that site. (A) all rain events and (B) close-up around threshold.

YBD1 and MBD1 only had one runoff event each in this analysis, and it occurred during the same rain event on 7/13/12 (Figure 5.3, 5.9). The total storm depth at YBD1 during this storm was 63.8 mm, and the no-flow rain event with the next largest total depth rained 29.2 mm, creating the large and high range for the YBD1 total depth threshold (Table 5.8 and Figure 5.10). The mean of this depth threshold was 46.5 mm. At YBD1 the I60 runoff threshold mean, between the flow event with an I60 of 63.8 mm hr⁻¹ and the highest no-flow rain event with an I60 of 28.2 mm hr⁻¹, was 46.0 mm hr⁻¹, which has a 50-year recurrence interval according to the NOAA atlas for Yuma Proving Ground station, site ID: 02-9654 (Table 5.8 and Figure 5.5, 5.9). At MBD1 the total depth runoff threshold was from the runoff-producing

rain event with a total depth of 18.3 mm and the 16.3 mm total depth of the no-flow event (Table 5.8). The mean of this total depth runoff threshold range was 17.3 mm. The I60 runoff threshold mean was 7.5 mm hr⁻¹, which had a recurrence interval of less than one year, and was between the flow producing event with an I60 of 9.1 mm hr⁻¹ and the no-flow event with an I60 of 5.8 mm hr⁻¹ (Table 5.8 and Figure 5.5). During the runoff-producing rain event on 7/13/12, the MBD1 rain gauge had much lower rain depth and intensity than the other rain gauges in the watershed (Figure 5.1 and 5.2), so the threshold identified at this site may not be a good representation of the rain characteristics that generated runoff in this watershed. There were two flows at MIA1, and one of them was also during the large rain event on 7/13/12 (Figure 5.3). The total depth runoff threshold range at MIA1 was between the large rain event's total depth of 70.9 mm and the next highest magnitude of a no-flow producing event with a total depth of 30.7 mm (Table 5.8). The mean depth threshold was 50.8 mm. The I60 threshold range was between the large rain event's I60 of 62.7 mm hr⁻¹, which has a 100-200-year recurrence interval, and 23.9 mm hr⁻¹ (Table 5.8 and Figure 5.5). The mean of the I60 threshold was 43.3 mm hr⁻¹, with a 50-year recurrence interval. The other flow event at MIA1 was below this threshold. The depth and I60 of that rain event at MIA1 were 1.5 mm and 1.5 mm hr⁻¹, respectively.

6. DISCUSSION

6.1. *Runoff thresholds*

6.1.1. *Channels <3 km²*

In headwater channels, initiation of runoff from the piedmont surfaces relates to the hydraulic conductivity of the desert pavement, evaporation, and surface storage. McDonald et al. (2004) found that the A horizon of the desert pavement at YPG has a mean hydraulic conductivity of 6 mm hr⁻¹ when the matric potential is -2 cm. I60 thresholds for runoff in Piedmont Headwater (PH) channels are right around that hydraulic conductivity value, at 5.0 to 8.5 mm hr⁻¹. Less information is available about hydraulic conductivities of bedrock surfaces, but similar threshold ranges to those of PH channels suggest that hydraulic conductivities are also low for these sites. In addition to the influence of hydraulic conductivity on runoff initiation, other processes may also affect whether rain water reaches channels. Early rainfall may be slow to runoff due to higher infiltration and evaporation at the onset of a rain event. The shrink-swell eolian fines of the A-horizon have a higher infiltration rate when dry, and in some cases the initial high air and soil temperatures during the onset of a rainstorm are likely to cause evaporation of water falling on these surfaces. The surface of the piedmont is relatively flat, but some areas may also allow ponding and surface detention storage.

The range and mean of the five channel types' basin area size and the range and mean of the mean I60 threshold for each site is illustrated in Figure 6.1 A and B, respectively. The mean I60 of a rain event to cause runoff increased with increased basin area for Piedmont Headwater (PH), Bedrock (BK), and Bedrock with Alluvium (BA) channel types. The channel length increases with increased catchment area (Table 3.2), so this trend applies to channel length for these three channel types as well. When thresholds are plotted against catchment area, the I60 thresholds increased with the log of catchment

areas for catchments $<3 \text{ km}^2$ (Figure 6.2). This relationship is related to differences in runoff generation and channel flow with changing contributing area. The low rain intensity runoff thresholds at the headwater channel types, BK and PH, are due to their low infiltration rate and small catchment areas. Excess-overland flow initiates as the rain intensity exceeds the infiltration rate, and because there is not much alluvium for subsurface detention or a large catchment area for surface detention, the water quickly flows downstream. As the catchment area, channel width and length, and channel alluvium increase, both potential for detention storage and channel transmission losses increase, which means that higher runoff must be generated to enable channel flow to reach downstream locations. Higher precipitation thresholds are needed to produce this increased channel flow. While a somewhat linear relationship develops between log catchment area and thresholds up to catchments of around 3 km^2 , this relationship breaks down for larger catchments. This is due to both the location of stream monitoring relative to tributary inflows and the percentage of the storm coverage to catchment area decreasing as catchment area increases, so single rain gauges are no longer good indicators of catchment-scale precipitation.

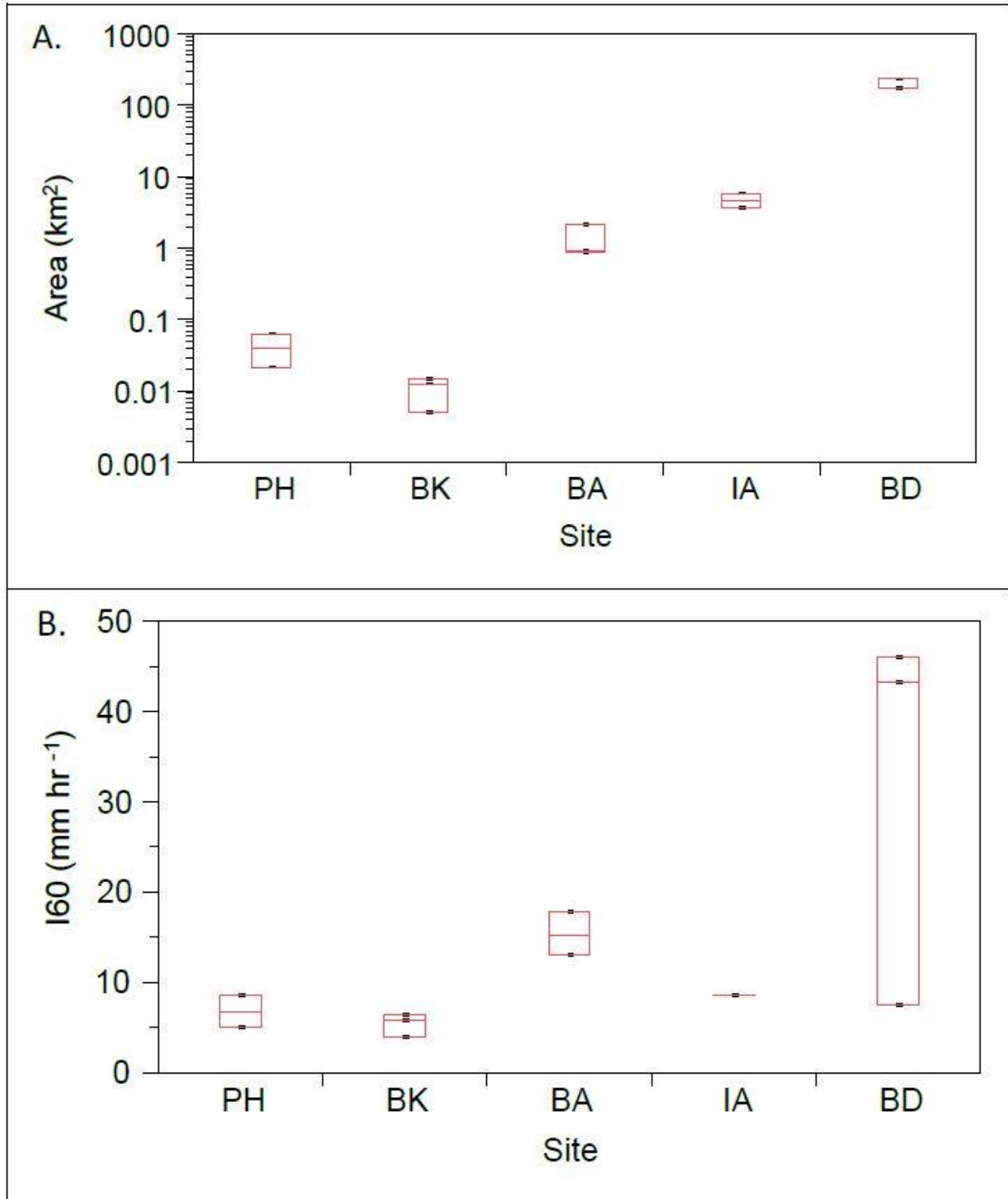


Figure 6.1. Box plots with data points of (A) basin area (y-axis in log scale) (Table 3.2) and (B) the mean of the I60 threshold range for all the sites analyzed in each stream type (Table 5.8). There was only one IA channel site that experienced flow, so there is only one data point.

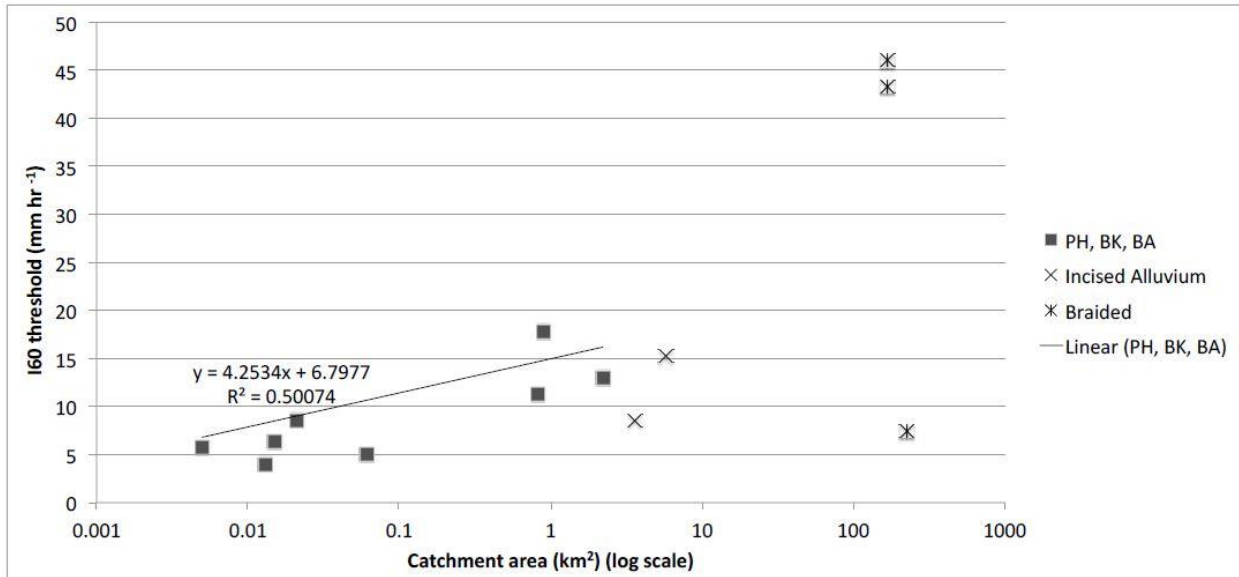


Figure 6.2. I60 threshold versus catchment area. The X-axis is in log scale. PH, BK, and BA sites are plotted as one group (solid boxes) with a linear trend line illustrating the linear increase of the I60 threshold with a log increase of the catchment area for these channel types. IA (Xs) and BD (stars) channel types are plotted as separate groups.

6.1.2. Incised Alluvium channels

Only one Incised Alluvium (IA) site, YIA1, had runoff, so there is only one data point in Figure 6.1.B for the IA channels. The lowest I60 rain event to cause flow at YIA1 was much lower than expected for a channel type with this size of basin area if there is a linear runoff response relationship between catchment area and I60 (Figure 6.2). This runoff producing rain event at YIA1 occurred on 8/17/12 and had an I60 of 9 mm hr⁻¹ and a depth of 9 mm at YIA1 (Figures 5.1-5.3, 5.8). Flow was recorded at the two upstream sites, YBK1 and YBA1, which was expected since the rain event's I60 at the two sites was above the BK and BA I60 runoff threshold (Figure 5.3). The rain event had an I60 of 23 mm hr⁻¹ and a depth of 23 mm at YBA1, which is 1.6 km upstream from YIA1, and at YBK1, 1.7 km upstream from YIA1, the rain event had an I60 of 19 mm hr⁻¹ and a depth of 19 mm (Figures 5.1 - 5.2). These higher rain intensities upstream indicate that the rain event's I60 was great enough to produce flow on the piedmont surrounding YIA1 (Table 4.1, Figures 3.3, 4.1). Therefore, the flow at YIA1 is probably due to

inputs from upstream, where the rain event had a higher I60 and depth, and at YIA1 the inputs were probably also from surrounding piedmont surfaces that contributed more localized flows.

YIA1 has a PH tributary that contributes flow directly upstream of and on the same side of the channel as the pressure transducer (Figure 3.6), which lowers the flow producing I60 threshold at YIA1. At YIA1 there were two flow producing rain events that did not produce flow upstream at YBA1. These events, which occurred on 12/13/12 and 8/22/13, had I60s of 9 and 15 mm hr⁻¹ at YIA1, and I60s at YBA1 of 12 and 2 mm hr⁻¹, respectively. The I60s of the rain events at YIA1 were over the runoff threshold for the PH channels. YPH1, 1 km away, also had flow during the 8/22/13 event, but the pressure transducer was not recording during the 12/13/12 event. Because YIA1 and YPH1 had the same I60 threshold (Table 5.8), the localized flow at YIA1 was probably produced on the piedmont surfaces and input directly to YIA1. Hence the threshold at YIA1 is more representative of a PH threshold than an IA threshold.

The highest I60 rain event recorded at the YIA2 site was 15 mm hr⁻¹, and no flow was recorded at that site. A threshold at this site greater than 15 mm hr⁻¹ would be consistent with the increasing I60 thresholds for this site's catchment area of 5.7 km². YIA2 does not have a PH channel contributing directly to the site, so its flow contributions are from further upstream at YBK2 and YBA2 sites and would be subject to transmission losses as flow moves downstream to this site. The lack of flow at YIA2 and its higher threshold than YIA1 could be due to catchment area differences, such as a different basin area, different permeability of bedrock types, and different percentages of desert pavement. However, the proximity of the YIA1 monitoring site to a piedmont headwater channel inflow is probably the most significant factor contributing to the differences in thresholds between YIA1 and YIA2. The reason for no flow at YIA2 could also be that the rain gauge 1.4 km away did not record the correct precipitation characteristics for the YIA2 site. A rain gauge distance of 1.4 km may be too far away to give accurate information on precipitation within the contributing area.

6.1.3. Braided channels

The large threshold at YBD1 suggests that it takes a large rain event with a high I60 and depth in the watershed to produce flow this far downstream. The only recorded flow at YBD1 was on 7/13/12, the largest rain event during the study presented in section 5 (Figures 5.1-5.3). There was also one other flow at YBD1 on 8/17/12 when the rain gauge was not recording. There was flow at all monitoring sites during these two rain events, which suggests that in order for there to be flow recorded at YBD1, the majority of the basin must be contributing runoff. Otherwise, runoff is likely to be lost to channel transmission in the wide braided reaches.

The only flow recorded at MBD1 was also on 7/13/12 (Figure 5.3), but the rainfall at this location only had an I60 of 9.1 mm hr⁻¹ and a depth of 18.3 mm (Figure 5.1 - 5.2). The I60 and depth was much greater at other sites, and this storm produced flow in all the other monitoring sites. At MBA1 and MIA1 the I60 was 63 mm hr⁻¹ and the depth was 71 mm. The relatively low rainfall at MBD1 indicates that runoff at MBD1 largely depends on high rainfall in the contributing area. MIA1, which is grouped with braided channels based on contributing area, had two flow events. One was the event on 7/13/12, and the other was on 9/5/12 (Figure 5.3). For the 9/5/12 event, there was no flow and no rain at MBD1 (Figures 5.1-5.3), so whatever runoff passed through MIA1 on 9/5/12 had infiltrated before reaching MBD1. The I60 and depth for the 9/5/12 rain event at MIA1 was only 1.5 mm hr⁻¹ and 1.5 mm (Figure 5.1-5.2). In MBA1, which is a tributary to MIA1, there was no pressure transducer data during this event (it had not been replaced from washing away during the 7/13/12 flow event), though subsurface water content data indicated that flow did occur. However, this site too had low recorded rain with I60 and rainfall depth only 5.8 mm hr⁻¹ and 5.8 mm respectively. MIA1 has a large contributing area, and most of the basin is not instrumented with rain gauges, so it is likely that the flow event on 9/5/12 was due to rain in the ungauged part of the basin. These event examples at MIA1 and MBD1 show the importance of distributed monitoring of rain and runoff throughout the contributing areas of larger basins, as on-

site rain gauges for these channels may not be representative of the rain falling elsewhere in the contributing areas.

The BD channels have the largest basin area size and largest runoff threshold range. This large range indicates a large uncertainty in the threshold, if it exists. Only a limited number of flow events were recorded at these sites, but it is clear that the flow is not directly related to a local precipitation threshold. Occurrence of flow in both IA and BD sites depends largely on upstream inputs. A larger record of flow events and a denser network of rain gauges and pressure transducers are needed to define thresholds for larger contributing area channels with partial area coverage of storms. In this study, both the number of rain gauges and the length of record were insufficient to establish runoff thresholds for braided channels.

6.2. Runoff frequency

Runoff frequency logically should increase with smaller I60 thresholds, and the data show a steady increase in runoff frequency from BA to BK to PH channel types (Figure 6.3). PH and BK sites had very similar thresholds, with PH sites having slightly larger catchment areas (Tables 3.2, 5.8 and Figure 6.1-6.2) and higher thresholds. Higher I60 thresholds at PH sites should correspond with lower runoff frequency than at BK sites, but this pattern is not evident in Figure 6.3. It is possible that there are systematic differences in rain intensity characteristics between sites, as the bedrock sites tend to be at higher elevations. Another reason for the difference in frequency could be the time period that each site was active. YPH1 experienced the most data loss due to equipment failure, and a large percentage of data from 9/21/12 to 12/6/13 was lost. Also, YBK2 and MBK2 were installed in 3/30/13 and 2/9/13, respectively, compared to 11/12/11 for YBK1 and MPH1, and 3/14/12 for YPH1. YPH1 was active for most of the 2012 monsoon season but missed a large portion of 2013 monsoon season. YBK2 and MBK2 were active for the 2013 monsoon season but not the 2012 monsoon season. In Yuma Wash, there were

four recorded flow producing rain events during the 2012 monsoon season and only two during the 2013 monsoon season (Figure 5.1-5.3). In Mohave Wash, there were five flow producing rain events during the 2012 summer and four during the summer of 2013. Therefore, the reason PH sites had a larger runoff frequency than the BK sites could be due to the differences in runoff production between seasons when sensors were recording.

In the case of two of the PH and BK sites, MPH1 and YBK1, the time the sites were active does not explain why the PH sites had larger runoff frequencies than the BK sites, because they were both working most of the time between their installation until the end of the study, and they recorded roughly the same number of rain events (Table 5.3). MPH1 had a higher runoff percentage than YBK1, possibly because of location. Mohave Wash, with a total of 12 flow producing rain events during the study period, had more flow producing rain events than Yuma Wash, which had nine (Figure 5.1-5.3).

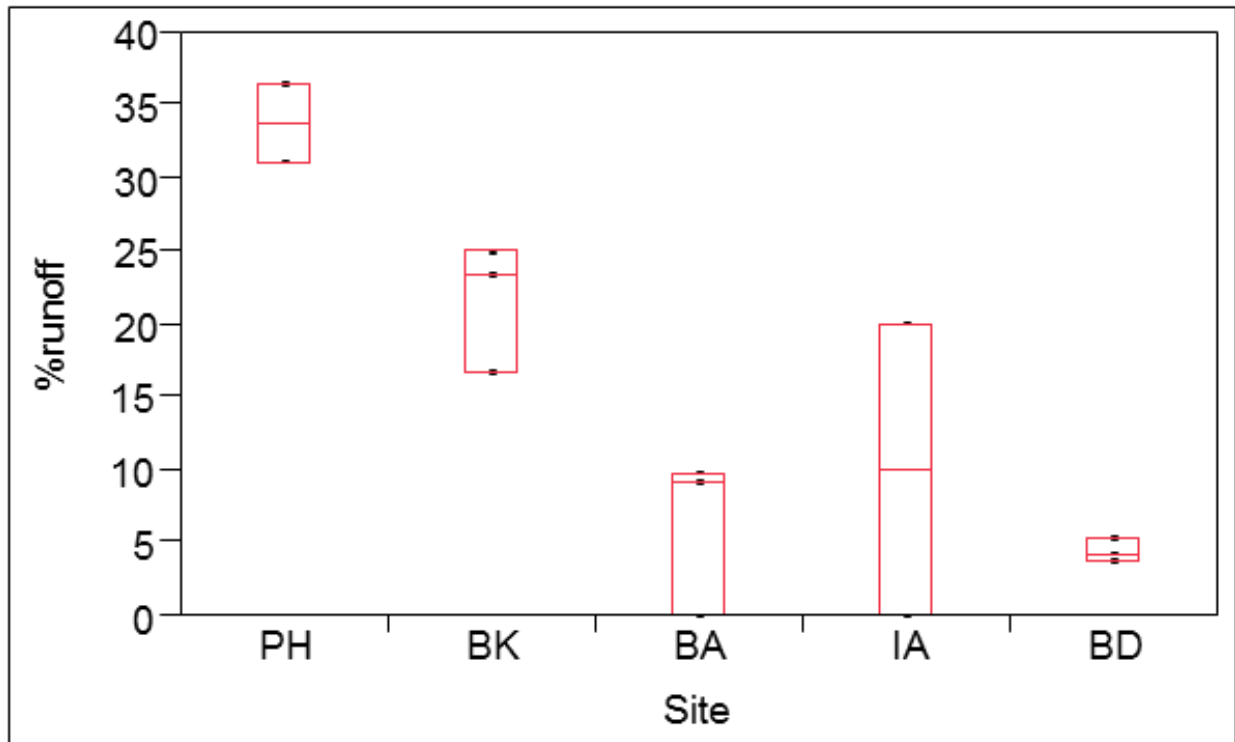


Figure 6.3. Box plots of percentage of rain events that produced runoff for each site grouped in the five channel types.

The BA sites had less frequent flows than PH and BK sites, and one BA site produced no flow (Figure 6.3). This relates to the higher I60 threshold to produce flow in these channels. As described for threshold changes with contributing area, lower frequency is expected in BA channels because as the catchment area increases, stream length and channel width increases, which increases the amount of channel alluvium and potential for transmission losses through longer lengths of channels (Goodrich et al 1997; Simanton and Osborn, 1983). Similarly, the lack of flow at YIA2 and the decreased flow frequency at the BD channels are also due to increased transmission losses with increasing drainage area. The large frequency range for the IA channels in Figure 6.3 is due to the 20% runoff frequency for YIA1. This larger than expected frequency at that site is attributed to the flow contributions from the tributary PH channel upstream of the pressure transducer. The three BD channels have a low runoff frequency and a small frequency range (Figure 6.3).

6.3. Uncertainty

Several factors contribute to uncertainties in the values of runoff thresholds defined for the study area. Uncertainties relate to rain event definition, seasonal differences in storm characteristics, and in associating correct rain characteristics with recorded runoff responses. This section describes some of the key uncertainties and how they affect the study results.

6.3.1. Minimum Inter-event Times (MIT)

Different minimum inter-event times (MIT) were tried in the rain event definition before 7 hours was selected for the final analysis. Increasing the MIT can lump multiple storms and reduce the number of rain events. The effects of MIT choice are most evident for small watersheds, where flow responds quickly to rain. At MPH1 a total of 35 rain events were recorded with an MIT of 2 hours, resulting in 229 mm depth of rain and 11 flow events. This gave a 31% flow frequency for the recorded time period. When the MIT was increased to 7 hours the total depth of rain increased to 231 mm because discarded

rain events less than 0.5 mm were lumped with other rain events. With the increase of MIT to 7 hours there were six fewer rain storms (35 to 29) and two fewer runoff events (11 to 9) because some storms less than 7 hours apart caused two distinct runoff events at MPH1. The longer MIT did not change the percentage of runoff events, but the depth threshold changed with a shorter MIT because the lowest depth to produce flow dropped to 7.4 mm instead of 8.9 mm. The lowest I60 to produce flow was 4.1 mm hr⁻¹, which did not change with a change in MIT. Since winter storms are usually long duration, low intensity storms, longer MITs can change the number of winter storms. It is possible that there should be a shorter MIT for the summer than for the winter, since these storms are so different in duration and intensity.

In some cases, the percentage of rain events that cause runoff can slightly change with a change in MIT. At YBK1 an MIT of 2 hours gave 32 rain events, and with an MIT of 7 hours there were 30 rain events. There were 7 runoff events regardless of MIT, which produced a runoff to rain event percentage of 21.9% for an MIT of 2 hours and 23.3% for an MIT of 7 hours.

6.3.2. *Winter storm effects*

Winter storms produced runoff at MPH1, YBK1, YBK2, and YIA1 (Table 5.4). BA and BD sites did not have winter flow, and with the exception of the one winter flow at YIA1, which was from local contributions to the channel from the surrounding piedmont surfaces, all other winter flows occurred in the headwater channel types. MPH1 and YBK2 had the highest percentage of winter storms causing runoff events (Table 5.4), and these are the only sites for which the precipitation depth metric was the only best choice for the runoff threshold (Table 5.6). The depth metric better accounts for the large total depth and low intensity rains of the winter months and is a better metric for runoff thresholds in winter storms in headwater channels.

While winter rain events helped to determine the threshold range at some headwater channels, they also created false positives and false negatives in threshold analysis. The large depth of winter storms decreased the I60 necessary for runoff production at headwater sites. In some cases this caused a runoff-producing winter storm to create a false negative in an intensity threshold analysis. Determining an intensity threshold can be complicated by winter storms if the intensity of a runoff-producing winter storm is just below a no-flow monsoonal storm near the intensity threshold. Using the winter storm's I60 for the threshold causes the monsoon storm to be a false positive, but using the monsoon event's I60 causes the winter storm to create a false negative. Though the depth metric was better for winter storms, it is possible that no-flow winter storms can cause false negatives because of their large depth when compared with low depth, high intensity storms that produced runoff during the monsoon season. In headwater channels seasonal metrics could help identify more accurate precipitation thresholds.

6.3.3. *Lag times*

The decision about whether or not a rain event is associated with a runoff response relates to the lag time between rain and runoff during each event. Lag times varied between storms and channel types, and in some cases, runoff would actually peak before rain. The lag between the rain event peak and the flow peak is due to multiple factors, including the distance between pressure transducer and rain gauge, the speed and direction of rain events, the speed of the flow downstream, and the runoff response time to precipitation. The flow response to water inputs at BK and PH channels is rapid, since overland flow develops quickly on the low permeable bedrock and piedmont surfaces. The headwater sites' flow response to the rain event on 7/13/12 (Figure 5.4) is a good example of how the combined movement of storm cells and runoff can affect interpretations of runoff responses. YBK1, which had a rain gauge on-site, had the smallest lag time, around 10 minutes, showing the quick runoff response of

headwater channels (Figure 5.4). Both flows at MPH1 occurred around an hour before it rained at the closest rain gauge 1.5 km away at MBD1 (Figure 5.4). The flow at YPH1 peaked around 15 minutes before the peak rain at its rain gauge at YIA1, only 1 km away. The flow occurring at these two PH sites before it rained at their nearest rain gauge shows the importance of having a rain gauge on-site in headwater catchments in order to measure runoff response times. Also, since the response time at these headwater sites can be less than 15-minutes, a temporal resolution greater than 15-minutes is necessary to determine actual lag times. In larger catchments, both storm speed and direction and channel flow speed contribute to the lag time between peak rain and peak runoff. For these catchments, a high spatial resolution of rain data may be needed to understand the source and timing of rain that generates runoff.

7. CONCLUSIONS

Precipitation thresholds for runoff generation were best defined for watersheds $<3 \text{ km}^2$, where rain intensity thresholds increased with the log of the catchment area. For larger catchments, spatial variability of storms in the contributing area means that thresholds are not well defined. Wide channels with large catchment areas can still experience small flows from low intensity rains if a headwater tributary contributes water directly into the channel near an observation location. However, this flow may not fill the whole width of the channel, and may not travel very far downstream due to channel bed transmission loss. Besides some uncertainty with Piedmont Headwater and Bedrock channel types, flow frequency increased with smaller I60 thresholds and decreased catchment area.

All four precipitation metrics – depth, I15, I30, and I60 – had an accuracy of at least 95.5% at identifying a runoff threshold. Overall, I60 was the best metric at predicting runoff. However, winter storm runoff thresholds were not always represented accurately with the I60 metric. At headwater channels, where runoff can be produced by long duration, low intensity winter storms, the depth metric sometimes worked better. For small headwater channels, identifying precipitation thresholds for runoff production may require different metrics for the two seasons: depth metric for winter rain events and I60 for summer rain events. The minimum inter-event time (MIT) used to define a storm event can also affect the threshold depth and flow frequency in small watersheds. A shorter MIT might be more appropriate for summer convective storms and a longer MIT for lower intensity winter frontal storms.

Although most runoff-producing rain events affected the entire study area, only one of these runoff-producing rain events led to runoff throughout the study channels; all other runoff events were localized, only in one or two sites, indicating discontinuous runoff through the channel network. Because of the spatial variability in rainfall and runoff, a dense network of rain gauges and flow monitoring devices with high temporal resolution is needed to understand fully the connections

between rainfall characteristics and runoff. Rain gauges on-site reduced uncertainty in lag times and showed that lag times at sites with small watersheds were less than half an hour. Because of the combination of storm movement and channel flow, densely spaced rain gauges are needed to capture accurate storm characteristics. Based on the runoff measurements that had to be excluded from this study, the density of rain gauges should be greater than one gauge per 1.5 km, with even closer spacing where there is substantial elevation change. Because of the rapid runoff response to rain, fine temporal resolution is needed for recording both precipitation and stage. The 15-minute resolution in this study was too coarse to capture the dynamics of these events.

While precipitation thresholds do not indicate runoff magnitude in ephemeral channels, they can be important tools for predicting flow in these systems, where measurements of stream discharge are rare and difficult to obtain. Advances in radar observations of rain patterns can be linked with runoff thresholds to identify when and where flash floods are likely to occur. The thresholds can also help to understand how flow frequency will be affected by changes of storm intensities due to climate change. This in turn can help predict the change in water regimes and plant available water in these ecosystems.

8. REFERENCES

- Arizona Geological Survey (AGS), 2000. Digital Geologic Map (DGM-17) (1:1,000,000-map scale).
http://www.azgs.az.gov/services_azgeomap.shtml
- Bonnin, G.M., Marin, D., Lin, B., Parzybok, T., Yekta, M., Riley, D., 2011. NOAA Atlas 14 Precipitation-Frequency Atlas of the United States, Volume 1 Version 5.0: Semiarid Southwest (Arizona, Southeast California, Nevada, New Mexico, Utah). U.S. Department of Commerce, National Oceanic and Atmospheric Administration, National Weather Service.
- Dunkerley, D., 2008. Identifying individual rain from pluviograph records: a review with analysis of data From an Australian dryland site. *Hydrological Processes*; 22:5024-5036.
- Goodrich, D. C., Lane, L. J., Shillito, R. M., Miller, S. N., Syed, K. H., Woolhiser, D. A. 1997. Linearity of basin response as a function of scale in a semiarid watershed. *Water Resources Research*; 33(12):2951-2965.
- Hallack-Alegria, M., and Watkins, D.W. Jr., 2007. Annual and Warm Season Drought Intensity-Duration-Frequency Analysis for Sonora, Mexico. *Journal of Climate*. American Meteorological Society; 27:1897-1909
- Hogan, J.F., Philips, F.M. and Scanlon, B.R. (Editors) 2004. Groundwater recharge in a desert environment: The southwestern United States. *Water Science and Applications Ser.9*. American Geophysical Union, Washington, DC
- Jaeger, K. L., and Olden, J. D., 2012. Electrical resistance sensor arrays as a means to quantify longitudinal connectivity of rivers. *River Research and Applications*; 28:1843-1852.
- Kidron, G.J., and Pick, K., 2000. The limited role of localized convective storms in runoff production in the western Negev Desert. *Journal of Hydrology* 229:281-289.
- Levick, L., J. Fonseca, D. Goodrich, M. Hernandez, D. Semmens, J. Stromberg, R. Leidy, M. Scianni, D. P.

- Guertin, M. Tluczek, and W. Kepner. 2008. The Ecological and Hydrological Significance of Ephemeral and Intermittent Streams in the Arid and Semi-arid American Southwest. U.S. Environmental Protection Agency and USDA/ARS Southwest Watershed Research Center, EPA/600/R-08/134, ARS/233046, 116 pp.
- McDonald, E., Hamerlynck, E., McAullife, J., and Caldwell, T. 2004. Analysis of desert shrubs along first-order channels on desert piedmonts: Possible indicators of ecosystem condition and historical variation. SERDP Seed project #CS1153, Final Technical Report.
- McFadden, L. D., Wells, S. G., Jercinovich, M. J., 1987. Influences of eolian and pedogenic processes on the origin and evolution of desert pavements. *Geology*; 15:504-508.
- Millennium Ecosystem Assessment, (2005) *Ecosystems and Human Well-being: Desertification Synthesis*. World Resources Institute, Washington, DC,
<http://www.millenniumassessment.org/documents/document.355.aspx.pdf>
- United States Department of Agriculture's Farm Service Agency's National Agriculture Imagery Program (NAIP), Aerial Photography Field Office, June 9, 2013.
- Osborn, H.B. 1964. Effect of storm duration on runoff from rangeland watersheds, in the semiarid southwestern United States. *International Association of Scientific Hydrology IX (4)*, 40-47.
- Osborn, H.B., and Lane, L.J., 1969. Precipitation-runoff relations for very small semiarid rangeland watersheds. *Water Resources Research* 5 (2), 419-425.
- Schreiber, H.A., and Kincaid, D.R., 1967. Regression models for predicting on-site runoff from short-duration convective storms. *Water Resources Research* 3(2), 389-395.
- Shaw, J. R., & Cooper, D. J. 2008. Linkages among watersheds, stream reaches, and riparian vegetation in dryland ephemeral stream networks, 68–82. doi:10.1016/j.jhydrol.2007.11.030
- Simanton, and J.R., Osborn, H.B., 1983. Runoff estimates for thunderstorm rainfall on small

- rangeland watersheds. Hydrology and Water Resources in Arizona and the Southwest. Proceedings of the 1983 Meetings of the Arizona Section, American Water Resources Association and the Hydrology Section, Arizona, Nevada Academy of Sciences, Flagstaff, Arizona, April 16.
- Springer, M.E., 1958. Desert Pavement and Vesicular Layer of Some Soils of the Desert of the Lahontan Basin, Nevada. Soil Science Society of America Journal. Soil Science Society Proceedings. 22(1), 63-66.
- Sutfin, N.A., Shaw, J., Wohl, E.E., Cooper, D., 2014. A geomorphic classification of ephemeral channels in a mountainous, arid region, southwestern Arizona, USA. Geomorphology, 221:164-175.
- Syed, K. H., Goodrich, D. C., Myers, D. E., & Sorooshian, S. 2003. Spatial characteristics of thunderstorm rainfall fields and their relation to runoff. Journal of Hydrology, 271:1–21.
doi:[http://dx.doi.org/10.1016/S0022-1694\(02\)00311-6](http://dx.doi.org/10.1016/S0022-1694(02)00311-6)
- Turk J K, Graham R C. 2011. Distribution and Properties of Vesicular Horizons in the Western United States. Soil Science Society of America journal; 75(4):1449-1461.
- Western Regional Climate Center. Yuma Proving Ground (029654), Period of record monthly climate summary: <http://www.wrcc.dri.edu/cgi-bin/cliMAIN.pl?az9654>. Accessed 18 June 2013.
- Wilcox, B.P., Newman, B.D., Brandes, D., Davenport, D.W., Reid, K. 1997. Runoff from a semiarid ponderosa pine hillslope in New Mexico. Water Resources Research, 33(10):2301-2314.
- Yair, A., and Lavee, H., 1985. Runoff generation in arid and semi-arid zones. Hydrological Forecasting, edited by M.G. Anderson and T.P. Burt. John Wiley, New York, 183-220.
- Young, M.H., McDonalds, E.V., Caldwell, T.G., Benner, S.G., Meadows, D.G., 2004. Hydraulic properties of a desert soil chronosequence in the Mohave desert, USA. Vadose Zone Journal 3:956-963.